Documento de Trabajo 2000-09

SMOOTHNESS, DEGREES OF FREEDOM AND LIAPUNOV EXPONENTS OF A TIME SERIES

Mª Eugenia MERA RIVAS
Manuel MORÁN CABRE

FACULTAD DE CIENCIAS ECONOMICAS Y EMPRESARIALES
UNIVERSIDAD COMPLUTENSE DE MADRID
VICEDECANATO
Campus de Somosaguas, 28223 MADRID. ESPAÑA.

SMOOTHNESS, DEGREES OF FREEDOM AND LIAPUNOV EXPONENTS OF A TIME SERIES

Mª Eugenia MERA RIVAS

Manuel MORÁN CABRE

Smoothness, degrees of freedom and Liapunov exponents of a time series.

M. Eugenia Mera. Manuel Morán.

October 14, 1999

Abstract

We propose a set of tests addressing the issue of determining whether the generating law of a time series is a stochastic process or a chaotic dynamics. In the latter case, we test the smoothness and find the number of degrees of freedom of the underlying dynamics. We propose an adaptation of Eckmann and Ruelle algorithm for the computation of the Liapunov exponents of a time series. This algorithm computes efficiently the whole Liapunov spectrum of the observed dynamics, avoiding the problem of the spurious exponents.

PACS 05.45.-a, 05.45 Tp, 05.10.-a

This research was partially supported by the Dirección General de Enseñanza e Investigación, PB97-0301.

Departamento de Análisis Económico I, Universidad Complutense, Campus de Somosaguas, 28223 Madrid. Spain.

E-mail: ececo06@sis.ucm.es

1 Introduction.

Eckmann and Ruelle devised an algorithm (E.R.A. for the sequel) to compute the Liapunov spectrum of the tangent map of a dynamical system (see [6]). This algorithm also works, via the time-delay method, for time series recorded from an observation of a smooth dynamical system. Taken's theorem guarantees (see [15]) that if the dynamics is defined in a smooth d-dimensional submanifold of IR^n, and the embedding dimension m is higher than $2d$, then

the series of m-histories is contained in a d-dimensional submanifold of IR^m. Moreover, Mera and Morán proved in [11] that if d is known, then it is possible to adapt E.R.A. to compute the complete Liapunov spectrum of the tangent map, avoiding the issue of the spurious exponents.

E.R.A. can process any time series, but the output of E.R.A. can be regarded as the asymptotic exponential rates of convergence or divergence of orbits with nearby initial conditions only when the time series is a smooth observation of an orbit of a smooth dynamical system. In consequence, the computation of the Liapunov spectrum of the tangent map of an observed dynamics should be preceded by two steps: a test for computing the dimension d of the submanifold, if any, where the original dynamics is defined, and a test of the smoothness of the forward shift of the m-histories.

We propose in section 2 an algorithm for the estimation of the dimension of the embedded submanifold. The algorithm is based on the analysis of the principal components of the distribution of the data points in small balls in the space of m-histories. If, for increasing values of m, the estimate of the dimension of the embedded submanifold becomes stabilized to a value D, this will be our estimate of the dimension d of the submanifold where the original dynamics is defined. If the algorithm always gives m as output then two alternative hypotheses are possible: either the series is generated by a stochastic law, or it is a projection of a higher dimensional dynamics in a lower dimensional space. In both cases the hypothesis of low dimensional chaos can be rejected and it does not make sense to compute the Liapunov spectrum of the tangent map with E.R.A. We give empirical evidence on the efficiency of this algorithm for the detection of stochastic noise, and for the estimation of the number d of degrees of freedom of a smooth dynamics on a d-dimensional submanifold whose Liapunov dimension Λ (see [5]) is larger than $d-1$ with $\Lambda - d + 1$ not too small. We also show that, for large enough time series, it is also possible, in principle, to detect hidden dimensions, linked to strongly negative Liapunov exponents, though the required length of the time series might render useless this method in most practical cases. However, even for short time series, the algorithm always provide a lower and an upper bound for the dimension d. Using the values D in between these bounds as estimates of the dimension, and studying the behaviour of the smoothness test, and the estimates of the Liapunov exponents using these values D, we can achieve the estimation of the dimension d of the submanifold even for short time series.

In section 3 we describe an algorithm to check the smoothness of the

forward shift of the m-histories. The algorithm is based on the analysis of the errors made by the best linear fittings to the action of the forward shift on small balls in the space of m-histories. It provides an efficient test to detect the differentiability of classical dynamical systems, and to reject the differentiability of samples of standard stochastic processes, in both cases even with not too long time series. We think that this test can provide an efficient alternative method to the techniques based on the correlation integral for checking whether the generating law of the time series is a smooth dynamical system.

Finally in section 4 we discuss the practical issues of the adaptation of E.R.A. for the estimation of Liapunov exponents of the tangent map in a smooth d-dimensional submanifold. We show that the convergence of this algorithm is not only a theoretical result. E.R.A. gives good estimates of all the Liapunov exponents if the time series is large enough. It also gives good estimates of the non negative exponents for not very large time series: around 1000 data points for two dimensional systems, and 5000 for three dimensional systems.

The Appendix is devoted to the proofs of the theorems giving a theoretical support to the algorithms proposed in sections **2** and **3.**

2 Estimation of the dimension of the submanifold.

In this section we undertake the issue of the numerical estimation of the degrees of freedom of an observed dynamics. Let $\{u_0, u_1, ..., u_{N-1}\}$ be a scalar time series obtained from a smooth observation of a smooth dynamics in a d-dimensional submanifold M of IR^n. Let $O_N^{(m)} := \{\mathbf{x}_i,\, i = 0, ..., N-m+1\}$ be a m-dimensional embedding of the observations, i.e.

$$\mathbf{x}_i := (u_i, u_{i+1}, ..., u_{i+m-1}).$$

Takens (see [15]) proved that if M is compact, and $m > 2d$, then generically $O_N^{(m)}$ is contained in a d-dimensional submanifold $\mathrm{J}_m(M)$ of IR^m, where J_m is an embedding diffeomorphism, and the same conclusion holds in the sense of prevalence under additional conditions on the dynamics (see [14]). Since the dimension of the tangent spaces $\mathrm{T}_{\mathbf{x}}(\mathrm{J}_m(M))$ of $\mathrm{J}_m(M)$ at any $\mathbf{x} \in \mathrm{J}_m(M)$ is also d, some algorithms for the estimation of d are based on the use of the embedded orbit $O_N^{(m)}$ to get a reliable estimate of the dimension of the

tangent spaces $\mathrm{T}_{\mathbf{x}_i}(\mathrm{J}_m(M))$ for $\mathbf{x}_i \in O_N^{(m)}$. The algorithm we propose obtains these estimates through the well known principal component analysis, used first to this end by Broomhead and King (see [1] and [2]).

Let N and m be fixed, $\mathbf{x}_i \in O_N^{(m)}$, and let $B(\mathbf{x}_i, r_0)$ denote the closed ball centered at $\mathbf{x}_i$ and with radius r_0. Let $V_{m,r_0}^{(i)}$ be the matrix with files $\mathbf{x}_j - \mathbf{x}_i$, $j \in \mathcal{N} := \{j : \mathbf{x}_j \in O_N^{(m)} \cap B(\mathbf{x}_i, r_0)\}$. If N is large, r_0 is sufficiently small, and $m > 2d$ then the vectors $\mathbf{x}_j - \mathbf{x}_i$ are approximate tangent vectors to the submanifold $\mathrm{J}_m(M)$ at the point $\mathbf{x}_i$. Therefore, they must approximately span a d-dimensional linear subspace, and the significative rank of $V_{m,r_0}^{(i)}$ must be d. The significative rank of $V_{m,r_0}^{(i)}$ coincides (see [7]) with the cardinality of the set of eigenvalues of the matrix $X_{m,r_0}^{(i)} := \left(V_{m,r_0}^{(i)}\right)^t V_{m,r_0}^{(i)}$ which are significantly non null (for a matrix A we are denoting by A^t the transposed matrix of A). The m *principal components* of the variables are defined as the eigenvectors of $X_{m,r_0}^{(i)}$ (see [7]).

For fixed r, let $\sigma_{m,r,j}^{(i)}$, $j = 1, ..., m$ be the eigenvalues of $X_{m,r}^{(i)}$ arranged in a decreasing ordering. We consider the average normalized eigenvalues,

$$\overline{\mathrm{VAR}}_{m,r,j} := \frac{1}{K} \sum_{i=0}^{K-1} \mathrm{var}_{m,r,j}^{(pi)}, \text{ where } \mathrm{var}_{m,r,j}^{(pi)} := \frac{\sigma_{m,r,j}^{(pi)}}{\sum_{j=1}^{m} \sigma_{m,r,j}^{(pi)}}, \qquad (1)$$

$j = 1, ..., m$, and p is the integer part of $(N - m + 1)/K$. These average normalized eigenvalues are averages of the percentages of the overall variability of the orbital measure distribution in small balls explained for each principal component (see [9]). Thus, we give as estimate D_m of the dimension of $J_m(M)$ the cardinality of the set of these values which are significantly non null.

We have implemented a FORTRAN code to obtain these estimates. In order to get independence of the results from the scale of measurement, the original time series is normalized to the interval $[0, 1]$. The entries of the code are the length N of the time series, the maximum embedding dimension $m_{\max}$, an initial radius $r_{\max} \leq 1$ and the value K considered in (1). We use the efficient search of neighbouring points provided by the box-assisted technique (see [8]), taking a length $r_{\max}$ for the side of the boxes. All the neighbouring points of a given point in dimension $m + 1$ stay in the set of neighbouring points in dimension m. This fact allows us to reduce the CPU time consumed in the search of neighbouring points. If for a given point $\mathbf{x}_{pi}$, dimension m and radius, there is not at least a number $\max\{6, 2m\}$ of neighbouring points, we discard this point and go on to the next point $\mathbf{x}_{p(i+1)}$, modifying conveniently the averaging weight $1/K$ in (1). For each m

$\in \{2, ..., m_{\max}\}$ and j, $1 \leq j \leq m$, we plot in a continuous line all the points $(r_i, \overline{\mathrm{VAR}}_{m,r_i,j})$ with $r_i = \frac{r_{\max}(50-i)}{50}$, $i = 0, ..., 49$ satisfying that for such radius r_i, the cardinality of discarded points does not exceed a 95% of K.

We have run the algorithm using time series from the smooth observation of orbits of the dynamical systems on *Table I* and also in time series from a sample of independent and identically distributed random variables with a Uniform distribution.

The results for a scalar time series $\{u_i, i = 0, ..., N-1\}$ from the Ikeda system are in *Fig.*1. The time series is obtained using the observable $h(x, y) = \ln(1 + x^2 + y^2)$, that is $u_i = \ln(1 + x_i^2 + y_i^2)$ where $\{(x_i, y_i), i = 0, ..., 49999\}$ are the first 50000 points of an orbit. There appear (see $1(a)$) three strips. The first two ones correspond to the average rates of the variability explained respectively by the first and second principal components, and the last strip corresponds to the average rates of the variability explained by the remaining principal components. The first two ones account almost all the variability of the data, respectively around a 67% and a 32%, so that the estimate D_m of the dimension of $J_m(M)$ must be at least two for any $m \geq 2$. In $1(b)$ we give an enlarged picture for the third principal component, which shows that $\overline{\mathrm{VAR}}_{m,r,3}$, $m \geq 3$ tend steadily to zero when r tends to zero, so that $D_m = 2$ for any $m \geq 2$. Thus the estimate of d we give is $D = 2$.

Fig. 2 corresponds to a scalar time series from a sample of 50000 points of a Uniform distribution in $[0, 1]$. For $m = 2$ the last principal component accounts a significative rate of the variability, so that the estimate of the dimension of $J_2(M)$ is $D_2 = 2$. This happens also for $m = 3$ so that the estimate of the dimension of $J_3(M)$ is $D_3 = 3$, and so on, reflecting the stochasticity of the process which generates the time series. Notice that a fast scarcity of neighbouring points for increasing values of m serves as indication that the data are not in a d-dimensional submanifold of IR^m for $d << m$. For instance, in *Fig.* 2 the curves for $m \in \{6, ..., 10\}$ do not appear due to a scarcity of points, and the curves for $m = 5$ are limited to the biggest values of the radius.

The procedure of taking a big initial radius $r_{\max}$ allows us to get an estimate of the dimension of M for shorter time series. This is illustrated in *Fig.* 3 where the dimension analysis is made for a time series of the Henon system using the observable $h(x, y) = x^2 + y^2$, a length $N = 5000$ and $r_{\max} = 0.2$. From the study of $3(a)$ we conclude that $D_m \geq 2$, for $m \geq 2$, and since the average rates of the variability explained by the third principal component tend to zero when r tends to zero (see $3(b)$), we give $D = 2$ as estimate of the dimension of the manifold where the original dynamics is

defined.

2.1 Hidden dimensions.

In this section we present the case when one or more degrees of freedom of a smooth dynamics are hidden due to the existence of strongly negative exponents which causes that the data points at small scales of observation appear as stretched along the linear span of the spatial directions corresponding to the unstable local manifold. This occurs for instance in the Lorenz and Rössler dynamics which are three dimensional dynamics with dimension of μ close to two. From a numerical point of view, this produces a near zero percentage of the overall variability explained by the third principal component rendering difficult to obtain a clear indication of the existence of the third dimension from the observed time series.

We illustrate this fact using the Lorenz dynamics (see *Fig.* 4). The results using a vectorial time series from an orbit of this system are shown in $4(a)$. This analysis has been made through a more simplified Fortran code that uses a vectorial time series instead of working with m-histories of a scalar time series for increasing values of m. The average normalized eigenvalues are denoted in this case by $\overline{\mathrm{VAR}}_{r,j}, j = 1, 2, 3$. The average proportion of the variability explained by the third principal component is very small, around a 2%. This causes difficulties to analyze from a scalar time series whether this variability remains positive. The results for a time series from the second coordinate of an orbit of the Lorenz system are shown in $4(b)$. There appear three strips around the approximate values 0.65, 0.32 and 0.03, corresponding to the average proportion of the overall variability explained respectively by the first, second, and remainder principal components. Since the average rates of the overall variability accounted by the second principal component are around a 33%, we can state that the dimension of the submanifold must be at least two. An enlarged picture of the average rates of the variability accounted by the third principal component can be seen in $4(c)$. Since they remain positive, the estimates D_m of the dimensions of $J_m(M)$ must satisfy $D_m \geq 3$ for any $m \geq 3$. However although the average rates of the variability accounted by the third principal component are positive, they are very small, and the rates accounted by the fourth one are smaller. Thus we need to know when these rates are sufficiently small as to provide an upper bound for the dimensions of $J_m(M)$.

In Theorem 1 of the Appendix we give a theoretical support to the following test: if M is a d-dimensional submanifold, then for $m > 2d$

$$\mathrm{LNVAR}_{m,r}(l) := \frac{\ln\left(\sum_{j=l+1}^{m} \overline{\mathrm{VAR}}_{m,r,j}\right)}{\ln r} > \gamma > 0 \iff d \leq l \qquad (2)$$

for any $K \in \mathrm{IN}$, a sufficiently large N, and a small r.

If N is not large, the scale of radii where there are available data is too small as to detect a clear slope in the graphs $(\ln r, \ln \sum_{j=l+1}^{m} \overline{\mathrm{VAR}}_{m,r,j})$. Thus, this test is useful only for large time series. Let j^* be the index satisfying that $\overline{\mathrm{VAR}}_{m,r,j^*} > 0$ and $\overline{\mathrm{VAR}}_{m,r,j^*+1} \sim 0$ for any small r. From (2) it follows that $d \geq j^*$ which is the criterion we have used at the beginning of this section. In order to get an upper bound for the dimension we take $l \geq j^*$, plot the points $(\ln r, \ln \sum_{j=l+1}^{m} \overline{\mathrm{VAR}}_{m,r,j})$ for a wide range of small radii r, and we consider the slope a_l of such curve as estimate of the fraction in (2). Thus, $a_l > 0$ implies $d \leq l$. Observe that this test provides a criterion to decide if the rate of convergence towards zero of the quantity $\overline{\mathrm{VAR}}_{m,r,j}$ is enough strong as to decide that $d \leq j - 1$.

We have designed a Fortran code for performing this test. The implementation seeks a compromise between the following requirements:
a) the accuracy in the estimates of $\overline{\mathrm{VAR}}_{m,r,j}$ $j = 1, ..., m$, which is achieved if the number $N_{\min}$ of neighbouring points in the balls of radius r is sufficiently large as to ensure that there are data points in the stable local manifold, and
b) a sufficient large range of radii where the curves $(\ln r, \ln \sum_{j=l+1}^{m} \overline{\mathrm{VAR}}_{m,r,j})$ $l \geq j^*$ show a well defined slopes. The smallness of the radii is required to guarantee that the embedded submanifold in balls of such radii admits a good approximation by the tangent space.

In order to obtain the averages $\overline{\mathrm{VAR}}_{m,r,j}$, $j = 1, ..., m$ over the same points for all the radii r, we select from the set of K points in (1) those with the property of having at least $N_{\min}$ neighbouring points in the ball of radius $r_{\min}$ for all the dimensions $m \leq m_{\max}$. The set of radii where we compute (2) is $R := \{r_j = r_{\min} + (100 - j)\frac{r_{\max} - r_{\min}}{100},\ j = 0, ..., 100\}$, where $r_{\min}$, $r_{\max}$ and $N_{\min}$ are entry parameters that must be chosen to guarantee *a*) and *b*).

We illustrate this test with a time series from the Lorenz dynamics. From the dimension algorithm we know that $D_m \geq 3$ for $m \geq 3$. In order to get a wide scale of radii we increase the length of the time series to $N = 2000000$ data points. We take $m \in \{7, ..., 10\}$ and plot in *Fig.* 4(*d*) the points $(\ln r_i, \ln \sum_{j=4}^{m} \overline{\mathrm{VAR}}_{m,r_i,j})$ for $r_i \in R$, where the parameter $r_{\min}$ is fixed at a value which gives at least a 12% of K as selected points. The estimate of the slope of such curves is positive so that $D_m \leq 3$ for $m \in \{7, ..., 10\}$ and therefore $D_m \leq 3$ for $m \leq 10$. This gives an estimate $D = 3$ for the dimension of M.

An analogous study for the Rössler dynamics is shown in *Fig.* 5. We have taken an orbit of this system and we have plotted the average rate of the variability explained by the three principal components in $5(a)$. As in the Lorenz dynamics the variability explained by the third principal component is very small, around a 0.47%, making very difficult to estimate the dimension d from an observed time series of this dynamics. *Fig.* $5(b)$ shows the average rates of the overall variability explained by each principal component in all the embedding dimensions in between 2 and 10, and we present an enlarged picture of the average rate of the variability explained by the third principal component for all the embedding dimensions in between 3 and 10 in $5(c)$. The study of theses figures give $D_m \geq 3$ for all $m \geq 3$, and since the slopes (see $5(d)$) of the curves $(\ln r_i, \ln \sum_{j=4}^{m} \overline{\mathrm{VAR}}_{m,r_i,j})$ for $r_i \in R$ and $m \in \{7,8,9,10\}$ are positive, we get an estimate $D = 3$ for the dimension of M.

Notice that, as in the Lorenz case, for $m \geq 7$ the slopes of the curves $(\ln r_i, \ln \sum_{j=4}^{m} \overline{\mathrm{VAR}}_{m,r_i,j})$ for $r_i \in R$ are greater than two. In Theorem **1** of Appendix it can be seen that this is the expected behaviour of a C^2 dynamics.

This algorithm can also be used for shorter time series, but in this case it only provides an upper and a lower bound for the dimension. The results for a time series of 5000 data points from the second coordinate of an orbit of the Lorenz system are shown in *Fig.* 6. From $6(a)$ and $6(b)$ we conclude that $D \geq 3$ and from $6(c)$ we get $D \leq 4$. In estimating $LNVAR_{m,r}(3)$, the curves $(\ln r_i, \ln \sum_{j=3}^{m} \overline{\mathrm{VAR}}_{m,r_i,j})$ do not show a clear positive slope, so we only can state that $D \in \{3,4\}$.

We will see later how to use the smoothness test, and the estimates of the Liapunov exponents given by E.R.A. in order to confirm the estimate of the dimension of the submanifold where a dynamics with hidden dimensions takes place.

3 Testing smoothness.

E.R.A. replaces the tangent maps at the points of the m-embedded orbit by the linear fits which best describes the action of the forward shift in small balls centered at these points. The test we propose is based on the study of the goodness of such linear fits for decreasing values of the radii of the balls, and it might also be useful as a previous test for forecasting algorithms based on linear fits, and for noise reduction.

Let d be the dimension of M, and let $O_N^{(m)}$ be an m-dimensional embedded orbit with $m > 2d$. Let $\mathbf{x}_i \in O_N^{(m)}$, let r be a small radius and $\mathcal{N} := \{j : \mathbf{x}_j \in O_N^{(m)} \cap B(\mathbf{x}_i, r)\}$. Since $O_N^{(m)} \subset \mathrm{J}_m(M)$, where $\mathrm{J}_m(M)$ is a d-dimensional submanifold of IR^m, the vectors $\mathbf{x}_j - \mathbf{x}_i$, $j \in \mathcal{N}$, cannot span IR^m. In fact, the

tangent map for the embedded dynamics at $\mathbf{x}_i$ is defined on $\mathrm{T}_{\mathbf{x}_i}(\mathrm{J}_m(M))$. Let $\widehat{\mathrm{T}}_i$ be an estimate of $\mathrm{T}_{\mathbf{x}_i}(\mathrm{J}_m(M))$, $j \in \mathcal{N}$, let $\mathrm{P}_{\widehat{\mathrm{T}}_i}(\mathbf{x}_j - \mathbf{x}_i)$ be the orthogonal projection of the vector $\mathbf{x}_j - \mathbf{x}_i$ onto $\widehat{\mathrm{T}}_i$. We give as estimate of the tangent map at $\mathbf{x}_i$ the linear map $S_{N,r,i}$ which best describes how the evolution law takes the vectors $\mathrm{P}_{\widehat{\mathrm{T}}_i}(\mathbf{x}_j - \mathbf{x}_i)$ to the vectors $\mathrm{P}_{\widehat{\mathrm{T}}_{i+1}}(\mathbf{x}_{j+1} - \mathbf{x}_{i+1})$, for $j \in \mathcal{N}$. That is, $S_{N,r,i}$ is the linear map which minimizes, in the set $\mathcal{L}(\mathrm{IR}^d)$ of linear maps $S : \mathrm{IR}^d \to \mathrm{IR}^d$, the mean square error

$$\mathbb{E}_{N,r,i}(S) := \frac{1}{\#\mathcal{N}} \sum_{j \in \mathcal{N}} \left(\left| \mathrm{P}_{\widehat{\mathrm{T}}_{i+1}}(\mathbf{x}_{j+1} - \mathbf{x}_{i+1}) - S\mathrm{P}_{\widehat{\mathrm{T}}_i}(\mathbf{x}_j - \mathbf{x}_i) \right|_2 \right)^2, \qquad (3)$$

where $\#\mathcal{N}$ denotes the cardinality of the set $\mathcal{N}$.

We take as estimate of $\mathrm{T}_{\mathbf{x}_i}(\mathrm{J}_m(M))$ the d-dimensional linear subspace $\widehat{\mathrm{T}}_i$ which best fits the data, in the sense that it minimizes the sum of the Euclidean distances between the vectors $\mathbf{x}_j - \mathbf{x}_i$ and $\widehat{\mathrm{T}}_i$, for $j \in \mathcal{Q}$, where $\mathcal{Q}$ is the set of indexes j corresponding to the N_{T} data points $\mathbf{x}_j$ in $O_N^{(m)}$ closest to $\mathbf{x}_i$, and N_{T} is a fixed value with $N_{\mathrm{T}} >> d$. It is known (see [4]) that $\widehat{\mathrm{T}}_i$ is the linear subspace spanned by the d eigenvectors corresponding to the d largest eigenvalues of the matrix $X^{(i)} := \left(V^{(i)}\right)^t V^{(i)}$ where $V^{(i)}$ is the $(N_{\mathrm{T}} \times m)$ matrix whose files are the coordinates of the points $\mathbf{x}_j - \mathbf{x}_i$, $j \in \mathcal{Q}$.

Let G_i be the orthonormal basis of $\widehat{\mathrm{T}}_i$ given by the eigenvectors of $X^{(i)}$, and let B_i be the $d \times m$ matrix whose files are the coordinates of the vectors of G_i expressed in the canonical basis of IR^m. Then, B_i is the matrix of the orthogonal projection $\mathrm{P}_{\widehat{\mathrm{T}}_i} : \mathrm{IR}^m \to \widehat{\mathrm{T}}_i$ expressed with respect to the canonical basis of the original space IR^m and with respect to the orthonormal basis G_i of the image space $\widehat{\mathrm{T}}_i$. Therefore, the matrix of the linear map $S_{N,r,i}$ expressed with respect to the orthonormal basis G_i and G_{i+1} is the $d \times d$ matrix which minimizes the expression

$$\mathbb{E}_{N,r,i}(S) := \frac{1}{\#\mathcal{N}} \sum_{j \in \mathcal{N}} (|B_{i+1}(\mathbf{x}_{j+1} - \mathbf{x}_{i+1}) - SB_i(\mathbf{x}_j - \mathbf{x}_i)|_2)^2. \qquad (4)$$

The test we propose is based on the quantity

$$R_{N,r} := \frac{1}{K} \sum_{i=0}^{K-1} \left[\mathbb{E}_{N,r,i}(S_{N,r,i}) \right]^{1/2}, \qquad (5)$$

which gives the average of the mean error made by the linear maps $S_{N,r,i}$ along the first K points of the orbit. In Theorem 2 of Appendix it is proved that under suitable conditions

$$\mathrm{R} := \liminf_{r \downarrow 0} \lim_{N \to \infty} \frac{\ln \mathrm{R}_{N,r}}{\ln r} \geq \delta$$

holds, where $\delta < 1$ for a Hölder dynamics, $\delta = 1$ for a continuously differentiable dynamics, and $\delta = 1 + \varepsilon$ for a $C^{1+\varepsilon}$ dynamics. Thus, a slope less than 1 in the curve $(\ln r, \ln \mathrm{R}_{N,r})$, gives an evidence of nondifferentiability of the observed dynamics.

At the beginning of this section we have assumed that d is the dimension of M. If d is unknown, we replace it by the estimate D obtained from the analysis of Section 2. Notice that if the dimension algorithm does not stabilize at a value D, and it always gives $D_m = m$ as the estimation of the dimension of $\mathrm{J}_m(M)$, then either the series is generated by a stochastic law, or it is a projection of a higher dimensional dynamics on a lower dimensional space. In both cases, the goodness of the best linear fits $S_{N,r,i}$, $i = 0, ..., K-1$ for the forward shift in the space of m-histories for any value of m is expected to be poor. To compute $S_{N,r,i}$ for $D = m$ we do not need to consider the projection onto the linear subspace that best fits the data points in small balls, so that the matrix of the linear map $S_{N,r,i}$ is the $m \times m$ matrix for which

$$\min_S \frac{1}{\#\mathcal{N}} \sum_{j \in \mathcal{N}} (|\mathbf{x}_{j+1} - \mathbf{x}_{i+1} - S(\mathbf{x}_j - \mathbf{x}_i)|_2)^2 \tag{6}$$

is attained. This is also the optimization problem which arises when we want to get the best linear fit for the action of the forward shift on a vectorial time series from an orbit of a dynamical system defined in an open subset of IR^m.

The test we propose also makes sense if $O_N^{(m)}$ is an orbit of a dynamical system defined in a smooth d-dimensional submanifold of IR^m instead of a reconstruction of a scalar time series. We have designed a Fortran code that covers this possibility allowing us to contrast the results of the smoothness test for orbits of known dynamical systems with those obtained using scalar time series from a smooth observation of these orbits.

For the general case the entries of the code are the length N of the time series, the embedding dimension m, the number K of fits, the dimension D where the linear fits are performed, an initial radius $r_{\max} \leq 1$ (as in the dimension algorithm, the original series is normalized to $[0, 1]$), and the number $N_{\mathrm{T}} >> D$ of points used for the estimation of the tangent spaces. Notice that if for a given radius r the average number of neighbours is near D, then $\mathrm{R}_{N,r}$ is near zero, but this goodness is due only to a scarcity of points. For this reason, we only add the terms $\mathbb{E}_{N,r,i}(S_{N,r,i})$ in (5) for the points $\mathbf{x}_i$ with at least a number $\max\{2D, D+4\}$ of indexes in $\mathcal{N}$, and we replace the averaging weight $1/K$ by $1/(K-Q)$ where Q is the number of points which do not satisfy this property.

The calculus of R_{N,r_j} is made for the radii $r_j = 2^{-\frac{j}{8}} r_{\max}$, $j = 0, ..., 48$. We

plot in a continuous line all the points $(\ln r_j, \ln \mathrm{R}_{N,r_j})$, $j = 0, ..., 48$ satisfying that for such radii r_j the number of discarded points does not exceed a 50% of K, and take as estimate of R the slope of such curve. The algorithm provides, for each radius, the number of discarded points, and also the average number of neighbouring points used for the estimation of the best linear fits. This allows us to evaluate the accuracy of the results.

We show the results for a vectorial time series from an orbit of the Lorenz system in *Fig.* 7(a). There appears a straight line with a slope equal to two, which reflects the differentiability of the dynamics. The figures 7(b) to 7(e) correspond to a scalar time series from this system obtained using the observable $h(x, y, z) = y$. Since this is a three dimensional system, we have taken as entry parameters $D = 3$ and $m \in \{3, ..., 8\}$. In all cases the data $(\ln r_i, \ln \mathrm{R}_{N,r_i})$ agree with a straight line, but for $m \in \{3, ..., 6\}$ (see 7(b)) the slopes are respectively around 0.95, 1.25, 1.3 and 1.55 so, they are lower than that obtained from the vectorial time series. For $m \in \{7, 8\}$ the slopes are respectively around 1.8 and 1.9 (see 7(c)). Thus, for any $m > 3$ the test gives as output values which strengthen the differentiability hypothesis. In order to illustrate that this method is also valid for short time series, we present in 7(d) an analysis analogous to that in 7(c) for a time series of 1000 data points. Again the results agree with the differentiability hypothesis, although the slope of the curves is slightly lower than before. In 7(e) we have set $m = D = 1$. The graph shows a line with a zero slope indicating the non differentiability of the forward shift due to the fact that the time series comes from the projection on IR of a higher dimensional dynamics. The results for $m = 7$ and $D \in \{1, 2, 3, 4, 5\}$ are shown in 7(f). The slopes of the curves for $D \in \{1, 2\}$ are close to one, and for $D \in \{3, 4, 5\}$ are close to two. Thus, although we can not reject the differentiability hypothesis for $D \in \{1, 2\}$, using that the slopes remain stabilized for $D \geq 3$, we must confirm the estimate $D = 3$ for the dimension of M obtained in Section 2.

Fig. 8 presents the results using a vectorial time series from an orbit of the Henon dynamics (see 8(a)) and the results for a scalar time series (see 8(b)) using the observable $h(x, y) = x^2 + y^2$. The results agree with the differentiability, and the slopes take the value 2 as in the vectorial time series case for any $m \geq 4$.

Fig. 9 shows the results for a scalar time series of 5000 points from a $N(0, 1)$ distribution. Since the dimension test gives always $D = m$ as the estimate of the dimension of the submanifold containing $O_N^{(m)}$, we have taken $m = D \in \{1, 2, 3\}$. In all cases the test rejects the differentiability hypothesis.

4 Adaptation of E.R.A. to the computation of the Liapunov exponents in smooth submanifolds.

Let d be the dimension of M, and let $m > 2d$. The adaptation of E.R.A. we propose (see [11]) takes the linear map $S_{N,r,i} \in \mathcal{L}(\mathrm{IR}^d)$ which solves (4) as estimate of the tangent map at $\mathbf{x}_i \in O_N^{(m)}$, instead of the linear map $S_{N,r,i} \in \mathcal{L}(\mathrm{IR}^m)$ which solves (6) as in E.R.A. algorithm. In this case, the algorithm provides only d exponents instead of the m exponents given by the standard E.R.A, thus avoiding the issue of the detection of the $m - d$ spurious exponents. The problem of the detection of the spurious exponents is also considered in [6] and [3]. The main difference between our method and the method considered in these papers is that in estimating the tangent map at $\mathbf{x}_i$ we project the tangent vectors $\mathbf{x}_j - \mathbf{x}_i$, and $\mathbf{x}_{j+1} - \mathbf{x}_{i+1}$, on the d-dimensional linear subspaces $\widehat{T}_i$ and $\widehat{T}_{i+1}$ close respectively to the tangent spaces $T_{\mathbf{x}_i}(J_m(M))$ and $T_{\mathbf{x}_i+1}((J_m(M))$, whilst in the quoted papers the tangent vectors at each point of the orbit are projected on the same d-dimensional linear subspace V. This has the potential drawback that if some orthogonal direction to V is close to the tangent space $T_{\mathbf{x}_i}(M)$ at some point $\mathbf{x}_i$ of the orbit, then a non negligible numerical error can occur in the estimation of the tangent map at $\mathbf{x}_i$.

Let $\alpha_{K,N,r,j}^{(m,d)}, j = 1, ..., d$ be the Liapunov exponents provided by the algorithm, obtained from an iterative QR decomposition of the $d \times d$ matrix $S_{N,r,K-1} \cdot S_{N,r,K-2} \cdots S_{N,r,1} \cdot S_{N,r,0}$, and assume that the Liapunov exponents of the tangent map λ_j, $j = 1, ..., d$ are well defined. Using the results of [11] and under the hypotheses of smoothness and regularity of the dynamics there explicited, it is easy to derive the convergence of the Liapunov exponents computed with E.R.A. from a time series to the Liapunov exponents of the tangent map, i.e. $\lim_{K\to\infty} \lim_{r\to 0} \lim_{N\to\infty} \alpha_{K,N,r,j}^{(m,d)} = \lambda_j, j = 1, ..., d$.

Since in practice d is unknown we replace it by the estimate D obtained through the dimension algorithm. It is also assumed that there is not evidence of non-differentiability of the m-reconstructed dynamics with $m > 2D$ (see Section 3). In order to get a higher accuracy in the estimation of Liapunov exponents, the best linear fit $S_{N,r,i}$ at $\mathbf{x}_i$ is obtained using only a fixed number $NV > D$ of the points in the ball $B(\mathbf{x}_i, r)$, corresponding to the NV closest neigbouring points. For the sequel we use the more simplified notation $\alpha_j^{(m,D)}$, $j = 1, ..., D$ for the estimates of the Liapunov exponents given by the algorithm for an m-dimensional reconstruction of a scalar time series,

using D as the dimension where the linear fits are performed, and for fixed values of the remainder parameters.

We have designed a Fortran code for the adapted E.R.A., which allows us to treat vectorial time series instead of reconstructions of scalar time series, so we can contrast the estimates α_j, $j = 1, ..., d$ of the Liapunov exponents obtained from an orbit of a known dynamical system with the estimates $\alpha_j^{(m,D)}$, $j = 1, ..., D$ using a scalar time series from the observation of such orbit. In the case that the tangent map is known, as in the Ikeda and the Henon dynamics, we also have the estimate of the Liapunov exponents given by the QR decomposition of the matrix obtained as the product of the tangent maps at the first K points of the orbit. We denote these estimates by $\lambda_{K,j}$, $j = 1, ..., d$.

The entry parameters of the code are the length of the time series N, the embedding dimension m, the dimension D where the fits are performed, the number $N_T >> D$ of neighbouring points used in the estimation of the tangent spaces, the number NV of neighbouring points required for each fit, and the number K of linear fits used in the estimation of the Liapunov exponents. As guidelines we do not consider an estimate of the Liapunov exponents as valid until we observe that it is stabilized for increasing values of K and N. Other useful test is to check the ergodicity hypothesis of the invariant measure by contrasting that the estimates do not depend on the initial point at which we begin to compute the best linear fits.

We show the results for a time series from the Henon system in *Table II*, for the entry parameters there specified. The results obtained from estimates of the tangent maps using an orbit of the system appear at the top of the table and they are denoted by $\alpha_i, i = 1, 2$. They are very close to the estimates obtained using the true tangent maps at the first K points of the orbit, which also appear at the top of the table and are denoted by $\lambda_{K,i}, i = 1, 2$. The results obtained from estimates of the tangent maps using a scalar time series, $m \in \{2, ..., 7\}$ and $D \in \{2, m\}$ are denoted by $\alpha_i^{(m,D)}$, $i = 1, ..., D$. These estimates are good for $D = 2$ and $m > 2$, even in the cases which are not covered by Takens's or Sauer's theorems. For $D = m \in \{3, ..., 7\}$ only the estimate of the positive exponent is good, and it is difficult to distinguish the true exponents from the spurious ones.

Table III shows the estimates of the Liapunov exponents provided by E.R.A. for a long and a short time series from Henon system. The estimates using an orbit of the system are very close to those obtained from the true tangent map even for the short time series, where we have the estimates $\alpha_1 = 0.4351$ and $\alpha_2 = -1.5684$. The results for a time series from the observation

of the system are accurate for the long time series, and any $m > 2$. For the short time series, the results are acceptable only for the positive exponent. In order to get a good estimate of the negative one, it is required to increase the length of the time series.

Table IV shows the estimates of the Liapunov exponents for the Ikeda system for a long and a short time series. As in the case of the Henon system, the results for the vectorial time series are good even for the short time series. In the scalar case, the estimates of the two exponents are accurate for the long time series and for any $m > 2$. For the short one, the estimates of the positive exponent are good for $m \in \{3, ..., 5\}$, and those of the negative exponent are quite good for $m \in \{4, 5, 6\}$. The estimates become poor when m increases due to a scarcity of neigbouring points which forces to increase the radii of the balls in order to get the NV neigbouring points required for the fits. Thus, when N is small we should give as estimates of the Liapunov exponents those obtained for $m = 2d + 1$, which is the smallest value guaranteeing that Taken's theorem holds.

Table V shows the results for the Lorenz system using $D = 3$ (at the top of the table) and $D = m$ (at the bottom of the table) as a function of m. It is known (see [3]) that $\lambda_1 \sim 1.50$, $\lambda_2 = 0$ and $\lambda_3 \sim -22.5$. For $D = 3$ the estimates are very good for any $m > 5$. For $D = m \in \{5, ..., 7\}$ the estimates are bad and it is very difficult to determine which should be the estimates of the true exponents.

Table VI shows the values obtained, for the Lorenz system, taking $D = 2$. If the dynamics was defined in a two dimensional submanifold, the estimates should remain stabilized near to the true values at least for $m > 4$. However, in this case the estimate of the first Liapunov exponent is almost stabilized only for $m > 8$, and the estimate of the second one requires still higher embedding dimensions. This gives an indication that the dynamics is defined in a submanifold of dimension greater than two. Thus, the dimension algorithm, the smoothness test, and the comparison of the estimates of the Liapunov exponents for $D = 2$ and $D = 3$ allow us to confirm that the dimension of the submanifold where the original dynamics is defined is equal to three.

We show in *Table VII* and *Table VIII* the results for scalar time series from the Lorenz and Rössler dynamics as a function of the length of the time series. It is known that the Liapunov exponents of the Rössler dynamics are (see [13]) $\lambda_1 \sim 0.069$, $\lambda_2 = 0$ and $\lambda_3 \sim -4.978$. The results for the long time series are very good for $m > 6$ in the Lorenz dynamics, and quite good for $m > 3$ in the Rössler dynamics. For a shorter time series the estimates of the largest Liapunov exponent are acceptable only when $N \geq 5000$ and $m \geq 7$. We present in these tables the results for a length of $N = 5000$.

5 Appendix

We start giving some definitions and notation. We say that a Borel probability measure μ on $M \subset \mathrm{IR}^n$ is *α-exact dimensional* if

$$\lim_{r \downarrow 0} \frac{\log \mu(B(\mathbf{x}, r))}{\log r} = \alpha \ \mu\text{-a.e. } \mathbf{x} \in M.$$

Let $\dim(A)$ denote the Hausdorff dimension of the set A (see [10]). The *Hausdorff dimension* of the measure μ is

$$\dim \mu := \inf\{\dim(A) : \mu(A) > 0\}.$$

Given $f : M \to M$, we denote by $O_N(\mathbf{z})$ the N first points of the orbit of $\mathbf{z} \in M$, and by μ_N the corresponding orbital measure, that is $\mu_N := \frac{1}{N} \sum_{i=0}^{N-1} \delta_{f^i(\mathbf{z})}$. The weak convergence of the sequence of measures $\{\mu_N\}$ to a measure μ is denoted by $\mu_N \xrightarrow{w} \mu$, and the support of a measure μ by $spt(\mu)$. We denote by $\mu|A$ the restriction of the measure μ to the set A, and by $g_{\#}\mu$ the measure induced by μ under the mapping g, that is $g_{\#}\mu(A) = \mu(g^{-1}(A))$. The set of k-dimensional linear subspaces of IR^n is denoted by $G(n,k)$, and the orthogonal projection of IR^n onto $\mathrm{T} \in G(n,k)$ is denoted by P_{T}.

Theorem 1 *Let M be a $C^{1+\varepsilon}$ d-dimensional submanifold of IR^n, let f be a measurable dynamics on M, and let μ be an f-invariant, ergodic and α-exact dimensional Borel probability measure on M with $\alpha > d-1$. Let $\mathbf{z} \in M$, $\mathbf{x}_i \in O_N(\mathbf{z})$, $r > 0$, and $X^{(i)}_{N,r} := \left(V^{(i)}_{N,r}\right)^t V^{(i)}_{N,r}$, where $V^{(i)}_{N,r}$ is the matrix which has as files the coordinates of the vectors $\mathbf{x}_j - \mathbf{x}_i$ with respect to an arbitrarily chosen orthonormal basis of IR^n, with the index j ranging in the set $\mathcal{N} := \{j : \mathbf{x}_j \in O_N(\mathbf{z}) \cap B(\mathbf{x}_i, r)\}$. Let $\sigma^{(i)}_{N,r,1} \geq \cdots \geq \sigma^{(i)}_{N,r,n}$ be the eigenvalues of $X^{(i)}_{N,r}$,*

$$\mathrm{var}^{(i)}_{N,r,j} := \frac{\sigma^{(i)}_{N,r,j}}{\sum_{l=1}^{n} \sigma^{(i)}_{N,r,l}}, \ j = 1, ..., n, \ \textit{and}$$

$$\gamma_k := \liminf_{r \downarrow 0} \lim_{N \to \infty} \frac{\log\left(\sum_{j=k+1}^{n} \mathrm{var}^{(i)}_{N,r,j}\right)}{\log r}, \ k = 0, ..., n-1.$$

Then the following implications hold μ-a.e. $\mathbf{z}$,

$$k \geq d \Longleftrightarrow \gamma_k > 0.$$

To prove this theorem we need the next lemma.

Lemma 1 *Let μ be a Borel probability measure on $M \subset \mathrm{IR}^n$. Let $\mathbf{x} \in spt(\mu)$, $k \in \{0, 1, ..., n-1\}$ and let $\mathrm{T}_{k,r}$ be the subspace where the minimum, over the set $G(n,k)$, of*

$$\mathrm{E}_{r,\mathbf{x}}(\mathrm{T}) := \int_{B(\mathbf{x},r)} (|\mathbf{y} - \mathbf{x} - \mathrm{P}_{\mathrm{T}}(\mathbf{y} - \mathbf{x})|_2)^2 \, d\mu(\mathbf{y}),$$

is attained, where P_{T} denotes the orthogonal projection of IR^n onto $\mathrm{T} \in G(n,k)$. Let B be an arbitrary orthonormal basis of IR^n, and let X_r be the matrix with (i,j) entry given by

$$\int_{B(\mathbf{x},r)} (y_i - x_i)(y_j - x_j) \, d\mu(\mathbf{y}),$$

where $y_i - x_i$ is the i-th coordinate of the vector $\mathbf{y} - \mathbf{x}$ with respect to B. Let $\sigma_{r,1} \geq \cdots \geq \sigma_{r,n}$ be the eigenvalues of X_r, and let $\mathbf{w}_{r,i}, i = 1, ..., n$ be the corresponding eigenvectors. Then
(i) $T_{k,r} = span\{\mathbf{w}_{r,1}, ..., \mathbf{w}_{r,k}\}$.
(ii) $\mathrm{E}_{r,\mathbf{x}}(\mathrm{T}_{k,r}) = \sum_{j=k+1}^{n} \sigma_{r,j}$.

Proof of Lemma 1. See the proof given in [4], Theorem 2, for discrete measures.

Remark 1 *Notice that, for $k = 0$, Lemma 1 gives*

$$\sum_{j=1}^{n} \sigma_{r,j} = \int_{B(\mathbf{x},r)} (|\mathbf{y} - \mathbf{x}|_2)^2 \, d\mu(\mathbf{y}).$$

Proof of Theorem 1. Let $\mathrm{T}_{N,k,r}$ be the subspace in $G(n,k)$ where the minimum of

$$\mathrm{E}_{N,r,i}(\mathrm{T}) := \int_{B(\mathbf{x}_i,r)} (|\mathbf{y} - \mathbf{x}_i - \mathrm{P}_{\mathrm{T}}(\mathbf{y} - \mathbf{x}_i)|_2)^2 \, d\mu_N(\mathbf{y})$$

is attained (recall that μ_N is the orbital measure). It is known (see [4] or Lemma 1) that

$$\mathrm{E}_{N,r,i}(\mathrm{T}_{N,k,r}) = \frac{1}{N} \sum_{j=k+1}^{n} \sigma_{N,r,j}^{(i)} \text{ and } \mathrm{T}_{N,k,r} = span\{ \mathbf{w}_{N,r,1}^{(i)}, ..., \mathbf{w}_{N,r,k}^{(i)}\},$$

where $\mathbf{w}_{N,r,j}^{(i)}$, $j = 1, ..., k$ are the eigenvectors corresponding to the first k eigenvalues of $X_{N,r}^{(i)}$.

Let $X_r^{(i)}$ be the matrix of Lemma 1 for the point $\mathbf{x}_i$ and the measure μ, let $\sigma_{r,1}^{(i)} \geq \cdots \geq \sigma_{r,n}^{(i)}$ be the eigenvalues of $X_r^{(i)}$, and let $\{\mathbf{w}_{r,1}^{(i)}, ..., \mathbf{w}_{r,n}^{(i)}\}$ be the corresponding eigenvectors. Using that M is a d-dimensional submanifold, $\partial B(\mathbf{x}_i, r)$ is an $n-1$ dimensional submanifold, and $\dim \mu > d-1$, we obtain that $\mu(\partial B(\mathbf{x}_i, r) \cap M) = 0$ for enough small r. This fact, together with $\mu_N \xrightarrow{w} \mu$ for μ-a.e. $\mathbf{z} \in M$, gives $\mu_N | B(\mathbf{x}_i, r) \xrightarrow{w} \mu | B(\mathbf{x}_i, r)$. Therefore $\lim_{N\to\infty} \frac{1}{N} X_{N,r}^{(i)} = X_r^{(i)}$ for μ-a.e. $\mathbf{z} \in M$ and any $\mathbf{x}_i \in O_N(\mathbf{z})$. Then, by the continuous dependence of the spectrum of a matrix upon its entries and Lemma 1 we have

$$\lim_{N\to\infty} \sum_{j=k+1}^{n} \mathrm{var}_{N,r,j}^{(i)} = \lim_{N\to\infty} \sum_{j=k+1}^{n} \frac{\sigma_{N,r,j}^{(i)}}{\sum_{l=1}^{n} \sigma_{N,r,l}^{(i)}} = \sum_{j=k+1}^{n} \frac{\sigma_{r,j}^{(i)}}{\sum_{l=1}^{n} \sigma_{r,l}^{(i)}} =$$

$$= \frac{\int_{B(\mathbf{x}_i,r)} \left(\left| \mathbf{y} - \mathbf{x}_i - \mathrm{P}_{\mathrm{T}_{k,r}}(\mathbf{y} - \mathbf{x}_i) \right|_2 \right)^2 d\mu(\mathbf{y})}{\int_{B(\mathbf{x}_i,r)} \left(|\mathbf{y} - \mathbf{x}_i|_2 \right)^2 d\mu(\mathbf{y})} \quad \mu\text{-a.e. } \mathbf{z} \in M,$$

where $\mathrm{T}_{k,r} = span\{\mathbf{w}_{r,1}^{(i)}, ..., \mathbf{w}_{r,k}^{(i)}\}$. Therefore

$$\gamma_k = \liminf_{r \downarrow 0} \frac{\log \left(\frac{\mathrm{E}_{r,\mathbf{x}_i}(\mathrm{T}_{k,r})}{\int_{B(\mathbf{x}_i,r)} \left(|\mathbf{y} - \mathbf{x}_i|_2 \right)^2 d\mu(\mathbf{y})} \right)}{\log r} \quad \mu\text{-a.e. } \mathbf{z} \in \mathrm{M}.$$

(i) We prove that $k \geq d$ implies $\gamma_k > 0$.
Let (U, ϕ) be a chart at $\mathbf{x}_i \in M$, where U is a neighborhood of $\mathbf{x}_i$, and ϕ is a $C^{1+\varepsilon}$ diffeomorphism on U such that $\phi(\mathbf{x}_i) = 0$. Since ϕ is $C^{1+\varepsilon}$ there exist constants L and r_0 such that $|\phi^{-1}(\mathbf{t}) - \phi^{-1}(0) - D\phi^{-1}(0)\mathbf{t}|_2 \leq L\left(|\mathbf{t}|_2\right)^{1+\varepsilon}$ holds if $|\mathbf{t}|_2 < r_0$. Furthermore for any constant K, with $K > \|D\phi(\mathbf{x}_i)\|_2$ there exists an $r_1 < \frac{r_0}{K}$ such that $|\phi(\mathbf{y}) - \phi(\mathbf{x}_i)|_2 \leq K |\mathbf{y} - \mathbf{x}_i|_2$ holds if $|\mathbf{y} - \mathbf{x}_i|_2 \leq r_1$. Let $\mathrm{T}_{\mathbf{x}_i}(M)$ denote the tangent space of M at $\mathbf{x}_i$. Let $r < r_1$, $\mathbf{y} \in \mathrm{B}(\mathbf{x}_i, r)$ and $\mathbf{t} = \phi(\mathbf{y})$. Then

$$\left| \mathbf{y} - \mathbf{x}_i - \mathrm{P}_{\mathrm{T}_{\mathbf{x}_i}(M)}(\mathbf{y} - \mathbf{x}_i) \right|_2 =$$
$$\left| \phi^{-1}(\mathbf{t}) - \phi^{-1}(0) - \mathrm{P}_{\mathrm{T}_{\mathbf{x}_i}(M)}(\phi^{-1}(\mathbf{t}) - \phi^{-1}(0)) \right|_2 \leq$$
$$|\phi^{-1}(\mathbf{t}) - \phi^{-1}(0) - D\phi^{-1}(0)\mathbf{t}|_2 \leq L\left(|\mathbf{t}|_2\right)^{1+\varepsilon} = L\left(|\phi(\mathbf{y}) - \phi(\mathbf{x}_i)|_2\right)^{1+\varepsilon} \leq$$
$$LK^{1+\varepsilon} r^{\varepsilon} |\mathbf{y} - \mathbf{x}_i|_2 ,$$

where the first inequality holds because $D\phi^{-1}(0)\mathbf{t}$ is a vector in $\mathrm{T}_{\mathbf{x}_i}(M)$. Thus $\mathrm{E}_{r,\mathbf{x}_i}(\mathrm{T}_{d,r}) \leq \mathrm{E}_{r,\mathbf{x}_i}(\mathrm{T}_{\mathbf{x}_i}(M)) \leq (LK^{1+\varepsilon} r^{\varepsilon})^2 \int_{B(\mathbf{x}_i,r)} \left(|\mathbf{y} - \mathbf{x}_i|_2 \right)^2 d\mu(\mathbf{y})$ for $r < r_1$, and therefore $\gamma_d \geq 2\varepsilon$ holds. If $k \geq d$ then $\mathrm{E}_{r,\mathbf{x}_i}(\mathrm{T}_{k,r}) \leq \mathrm{E}_{r,\mathbf{x}_i}(\mathrm{T}_{d,r})$

so that $\gamma_k \geq \gamma_d \geq 2\varepsilon$.

(ii) We prove that $\gamma_k > 0$ implies that $k \geq d$.
Assume that $k < d$. Since $\gamma_k > 0$, for any δ with $0 < \delta < \gamma_k$ there is an r_0 such that

$$\mathrm{E}_{r,\mathbf{x}_i}(\mathrm{T}_{d,r}) \leq \mathrm{E}_{r,\mathbf{x}_i}(\mathrm{T}_{k,r}) \leq r^{\gamma_k-\delta} \int_{B(\mathbf{x}_i,r)} (|\mathbf{y}-\mathbf{x}_i|_2)^2 \; d\mu(\mathbf{y}) \tag{7}$$

for $r < r_0$. Since μ is an α-exact dimensional measure, with $\alpha > d-1$, we can obtain an analogous result to that given in Theorem 2 of [12]: for any $\tau > 0$, and for μ-*a.e.* $\mathbf{x}_i \in M$ there are positive constants C, S and r_1, with $S < 1$ and $r_1 < r_0$, depending on $\mathbf{x}_i$ and on the chosen atlas of M, such that for any linear map $\beta \in \mathcal{L}(\mathrm{IR}^n)$

$$\|\beta\|_2 \leq \frac{C}{r^{1+\tau}} \left[\frac{1}{\mu(B(\mathbf{x}_i, Sr))} \int_{B(\mathbf{x}_i,r)} (|\beta(\mathbf{y}-\mathbf{x}_i)|_2)^2 \; d\mu(\mathbf{y}) \right]^{1/2} \tag{8}$$

holds for $r < r_1$. Taking τ with $0 < \tau < \frac{\gamma_k-\delta}{2}$, $\beta = \mathrm{P}_{\mathrm{T}_{d,r}} - \mathrm{P}_{\mathrm{T}_{k,r}}$ in (8), and using (7) we obtain

$$\left\| \mathrm{P}_{\mathrm{T}_{d,r}} - \mathrm{P}_{\mathrm{T}_{k,r}} \right\|_2 \leq$$

$$\frac{C}{r^{1+\tau}} \left[\frac{1}{\mu(B(\mathbf{x}_i,Sr))} \int_{B(\mathbf{x}_i,r)} \left(\left| (\mathrm{P}_{\mathrm{T}_{d,r}} - \mathrm{P}_{\mathrm{T}_{k,r}})(\mathbf{y}-\mathbf{x}_i) \right|_2 \right)^2 \; d\mu(\mathbf{y}) \right]^{1/2} \leq$$

$$\frac{C}{r^{1+\tau}(\mu(B(\mathbf{x}_i,Sr)))^{\frac{1}{2}}} \left[(\mathrm{E}_{r,\mathbf{x}_i}(\mathrm{T}_{k,r}))^{\frac{1}{2}} + (\mathrm{E}_{r,\mathbf{x}_i}(\mathrm{T}_{d,r}))^{\frac{1}{2}} \right] \leq 2Cr^{\frac{\gamma_k-\delta}{2}-\tau} \left(\frac{\mu(B(\mathbf{x}_i,r))}{\mu(B(\mathbf{x}_i,Sr))} \right)^{1/2}$$

for $r < r_1$. This inequality, together with the fact that μ is an exact dimensional measure, give that $\lim_{r\to 0} \left\| \mathrm{P}_{\mathrm{T}_{d,r}} - \mathrm{P}_{\mathrm{T}_{k,r}} \right\|_2 = 0$, which contradicts that $\mathrm{T}_{k,r} \in G(n,k)$ with $k < d$. ■

Remark 2 *Let* $\overline{\mathrm{VAR}}_{K,N,r,j} := \frac{1}{K} \sum_{i=0}^{K-1} \mathrm{var}^{(i)}_{N,r,j}$, $j = 1, ..., n$ *and*

$$\mathrm{LNVAR}_K(l) := \liminf_{r \downarrow 0} \lim_{N\to\infty} \frac{\log\left(\sum_{j=l+1}^{n} \overline{\mathrm{VAR}}_{K,N,r,j} \right)}{\log r}, \quad l = 0, ..., n-1.$$

Using that

$$\min_{0\leq i\leq K-1} \sum_{j=l+1}^{n} \mathrm{var}^{(i)}_{N,r,j} \leq \sum_{j=l+1}^{n} \overline{\mathrm{VAR}}_{K,N,r,j} \leq \max_{0\leq i\leq K-1} \sum_{j=l+1}^{n} \mathrm{var}^{(i)}_{N,r,j}$$

and Theorem 1 we have that

$$l \geq d \Longleftrightarrow \mathrm{LNVAR}_K(l) > 0$$

for any $K \in \mathrm{IN}$ *and for* μ*-a.e.* $\mathrm{z} \in M$, *which also implies* $\overline{\mathrm{VAR}}_{K,N,r,j} \sim 0$, *for any* $j > d$, *large* N, *and small* r. *This gives a theoretical support to the algorithm proposed in section 2.*

Theorem 2 *Let M be a d-dimensional smooth submanifold of IR^n, let f be a Borel measurable dynamics on M, and let μ be an f-invariant, ergodic and α-exact dimensional measure with $\alpha > d-1$. Let $\mathbf{z} \in M$, $\mathbf{x}_i \in O_N(\mathbf{z})$, $r_0 > 0$ and $\mathcal{N} = \{j : \mathbf{x}_j \in O_N(\mathbf{z}) \cap B(\mathbf{x}_i, r_0)\}$. Let $\widehat{\mathrm{T}}_i$ be the linear subspace where the minimum, in $G(n,d)$, of*

$$\mathrm{E}_{N,r_0,i}(\mathrm{T}) = \frac{1}{N}\sum_{j\in\mathcal{N}}(|\mathbf{x}_j - \mathbf{x}_i - \mathrm{P}_{\mathrm{T}}(\mathbf{x}_j - \mathbf{x}_i)|_2)^2$$

is attained. Let $S_{N,r,i}$ be the linear map where the minimum in $S \in \mathcal{L}(\mathrm{IR}^d)$ of

$$\mathbb{E}_{N,r,i}(S) := \frac{1}{\#\mathcal{Q}}\sum_{j\in\mathcal{Q}}(\left|\mathrm{P}_{\widehat{\mathrm{T}}_{i+1}}(\mathbf{x}_{j+1} - \mathbf{x}_{i+1}) - S\mathrm{P}_{\widehat{\mathrm{T}}_i}(\mathbf{x}_j - \mathbf{x}_i)\right|_2)^2$$

is attained, where $\mathcal{Q} := \{j \in \mathcal{N} : \mathrm{P}_{\widehat{\mathrm{T}}_i}(\mathbf{x}_j - \mathbf{x}_i) \in B(\mathbf{0}, r)\}$. Then

$$\mathrm{R}(K) := \liminf_{r\to 0}\lim_{N\to\infty}\frac{\log(\mathrm{R}_{N,r}(K))}{\log r}$$

where

$$\mathrm{R}_{N,r}(K) := \frac{1}{K}\sum_{i=1}^{K}(\mathbb{E}_{N,r,i}(S_{N,r,i}))^{\frac{1}{2}},$$

is defined μ-a.e. $\mathbf{z} \in M$ and for any $K \in \mathrm{IN}$. Furthermore
(i) If f is Hölder of exponent ε, then $\mathrm{R}(K) \geq \varepsilon$.
(ii) If f is Lipstchitz then $\mathrm{R}(K) \geq 1$.
(iii) If there is an $\varepsilon \in (0,1)$ such that $M \in C^{1+\varepsilon}$, and $f \in C^{1+\varepsilon}(M)$, then $\mathrm{R}(K) \geq 1+\varepsilon$.

Proof. It is not difficult to prove that for each $\mathbf{x}_i \in M$, there exists a neighborhood $U_{\mathbf{x}_i} \in \mathrm{IR}^n$, and a diffeomorphism $\Psi_{\mathbf{x}_i}$ defined in $U_{\mathbf{x}_i}$ such that the restriction of $\Psi_{\mathbf{x}_i}$ to $U_{\mathbf{x}_i} \cap M$ is given by $\Psi_{\mathbf{x}_i}(\mathbf{y}) = \mathrm{P}_{\widehat{\mathrm{T}}_i}(\mathbf{y} - \mathbf{x}_i)$. Thus, $(U_{\mathbf{x}_i}, \Psi_{\mathbf{x}_i})$ provides a chart at $\mathbf{x}_i$. Let $r_0 > 0$ such that $B(\mathbf{x}_i, r_0) \subset U_{\mathbf{x}_i}$, and $\nu_{N,i} := \Psi_{\mathbf{x}_i\#}(\mu_N | B(\mathbf{x}_i, r_0))$. Then,

$$\mathbb{E}_{N,r,i}(S) = \tfrac{1}{\nu_{N,i}(B(0,r))}\int_{B(0,r)}(|g_i(\mathbf{y}) - S\mathbf{y}|_2)^2\, d\nu_{N,i}(\mathbf{y})$$

holds, where $g_i := \Psi_{\mathbf{x}_{i+1}} \circ f \circ \Psi_{\mathbf{x}_i}^{-1}$. It can be proved that $S_{N,r,i}$ is defined for a sufficiently large N (see Lemma 1 and Theorem 2.3 in [11]). Using that $\mu_N \xrightarrow{w} \mu$, that $\Psi_{\mathbf{x}_i}$ is a diffeomorphism, and $\dim\mu > d-1$, we see that $\{\nu_{N,i} | B(0,r)\} \xrightarrow{w} \nu_i | B(0,r)$, where $\nu_i := \Psi_{\mathbf{x}_i}\#(\mu | B(\mathbf{x}_i, r_0))$. Since g_i is continuous

$$\lim_{N\to\infty}\mathbb{E}_{N,r,i}(S) = \mathbb{E}_{r,i}(S) \tag{9}$$

follows from the weak convergence, where

$$\mathbb{E}_{r,i}(S) = \frac{1}{\nu_i(B(0,r))} \int_{B(0,r)} \left(\left| g_i(\mathrm{y}) - S\mathrm{y} \right|_2 \right)^2 d\nu_i(\mathrm{y}).$$

Let $S_{r,i}$ be the linear map which minimizes $\mathbb{E}_{r,i}$ in $\mathcal{L}(\mathrm{IR}^d)$ (the existence and uniqueness of $S_{r,i}$ follows from Lemma 1 in [11]). Using that $\lim_{N\to\infty} S_{N,r,i} = S_{r,i}$ (the proof is as that given in Theorem 2.3 of [11]) and (9) we get

$$\lim_{N\to\infty} \mathbb{E}_{N,r,i}(S_{N,r,i}) = \mathbb{E}_{r,i}(S_{r,i}). \tag{10}$$

We first prove statement **(iii)**. If $M \in C^{1+\epsilon}$ and $f \in C^{1+\epsilon}(M)$ then $g_i \in C^{1+\epsilon}(\Psi_{\mathrm{x}_i}(U_{\mathrm{x}_i}))$, so that there is a constant L_i such that

$$|g_i(\mathrm{y}) - Dg_i(0)\mathrm{y}|_2 \leq L_i \left(|\mathrm{y}|_2\right)^{1+\epsilon} \tag{11}$$

holds for any $\mathrm{y} \in \Psi_i(U_{\mathrm{x}_i})$.

Since $S_{r,i}$ minimizes $\mathbb{E}_{r,i}$, we have that $\mathbb{E}_{r,i}(S_{r,i}) \leq \mathbb{E}_{r,i}(Dg_i(0))$ for any $i \in \mathrm{IN}$, which together with (10) and (11) gives that

$$\lim_{N\to\infty} \mathrm{R}_{N,r}(K) = \frac{1}{K} \sum_{i=1}^{K} \lim_{N\to\infty} [\mathbb{E}_{N,r,i}(S_{N,r,i})]^{\frac{1}{2}} = \frac{1}{K} \sum_{i=1}^{K} [\mathbb{E}_{r,i}(S_{r,i})]^{\frac{1}{2}} \leq$$

$$\frac{1}{K} \sum_{i=1}^{K} [\mathbb{E}_{r,i}(Dg_i(0))]^{\frac{1}{2}} \leq \frac{1}{K} \sum_{i=1}^{K} \left[\frac{1}{\nu_i(B(0,r))} \int_{B(0,r)} \left(L_i \left(|\mathrm{y}|_2\right)^{1+\epsilon} \right)^2 d\nu_i(\mathrm{y}) \right]^{1/2} \leq$$

$$\frac{r^{1+\epsilon}}{K} \sum_{i=1}^{K} L_i \leq L r^{1+\epsilon},$$

where $L = \max\{L_i : 1 \leq i \leq K\}$. Then $\liminf_{r\downarrow 0} \lim_{N\to\infty} \frac{\log(\mathrm{R}_{N,r}(K))}{\log r} \geq 1+\epsilon$. Parts **(i)** and **(ii)** are obtained using that $\mathbb{E}_{r,i}(S_{r,i}) \leq \mathbb{E}_{r,i}(0)$. ■

Acknowledgments. We are grateful to J.P. Eckmann for his support to this research.

References

[1] D.S. Broomhead and G.P. King. Extracting Qualitative Dynamics from Experimental Data, *Physica 20D*, (1986), 217-236.

[2] D.S. Broomhead and G.P. King. Phase Portraits from a Time Series: A Singular System Approach, *Nuclear Physics B*, **2**, (1987), 379-390.

[3] R. Brown, P. Bryan and H. Abarbanel. Computing the Liapunov spectrum of a dynamical system from an observed tieme series. *Physical Review A,* 43, (1991), 2787-2806.

[4] R. Cawley and Guan-Hsong Hsu. Local Geometric Projection Method for Noise Reduction in Chaotic Maps and Flows, *Physical Review A,* 46, 6, (1992), 3057-3082.

[5] J.P. Eckmann and D. Ruelle. Ergodic Theory of Chaos and Strange Attractors, *Reviews of Modern Physics,* 57, 3, (1985), 617-656.

[6] J.P. Eckmann, S.O. Kamphorst, D. Ruelle and S. Ciliberto. Liapunov Exponents from Time Series, *Physical Review A,* 34, 6, (1986), 4971-4979.

[7] P.E. Gill, W. Murray and M.H. Wright. Numerical Linear Algebra and Optimization. Volume 1. Addison-Wesley Publishing Company (1991).

[8] P. Grassberger. An Optimized Box-Assisted Algorithm for Fractal Dimensions, *Phys. Lett. A,* 148, (1990), 63-68.

[9] A. M. Kshirsagar. Multivariate Analysis. Marcel Dekker. NY (1972).

[10] P. Mattila. Geometry of Sets and Measures in Euclidean Spaces. Fractals and Rectifiability. Cambridge University Press (1995).

[11] M.E. Mera and M. Morán. Convergence of the Eckmann and Ruelle Algorithm for the Estimation of Liapunov Exponents, (forthcoming in *Ergodic Theory and Dynamical Systems*).

[12] M.E. Mera and M. Morán. $L^p(\mu)$-Estimation of Tangent Maps, *Journal of Mathematical Analysis and Applications* 235, (1999), 454-469.

[13] M. Sano and Y. Sawada. Measurement of the Lyapunov Spectrum from a Chaotic Time Series. *Physycal Review Letters,* 55, 10, (1985), 1082-1085.

[14] Sauer T., York J.A. and Casdagli M. Embedology. *Journal of Statistical Physics,* 65, 3/4, (1992), 579-616.

[15] F. Takens. Detecting Strange Attractors in Turbulence, *Dynamical Systems and Turbulence. Lectures Notes in Mathematics,* 898, 396, (1981).

TABLE 1

SYSTEM	EQUATIONS	Parameters Values.
(i) Henon	$x_{k+1} = 1 - ax_k^2 + y_k$ $y_{k+1} = bx_k$	$a = 1.4$ $b = 0.3$
(ii) Ikeda	$z_k = x_k + iy_k$ $z_{k+1} = p + Bz_k \exp\{\frac{i\omega - i\alpha}{1+\|z_k\|^2}\}$	$p = 1.0, \quad B = 0.9,$ $\omega = 0.4, \quad \alpha = 6.0$
(iii) Lorenz	$\frac{dx(t)}{dt} = -\sigma x(t) + \sigma y(t)$ $\frac{dy(t)}{dt} = -x(t)z(t) + rx(t) - y(t)$ $\frac{dz(t)}{dt} = x(t)y(t) - bz(t)$	$\sigma = 16$ $b = 4$ $r = 45.92$
(iv) Rössler	$\frac{dx(t)}{dt} = -y(t) - z(t)$ $\frac{dy(t)}{dt} = x(t) + ay(t)$ $\frac{dz(t)}{dt} = b + z(t)(x(t) - c)$	$a = 0.2$ $b = 0.2$ $c = 5.7$

Equations and parameter values of the dynamical systems used in this paper. Orbits for the continuous time systems are obtained using a fourth-order Runge-Kutta method with a integration time step $h = 0.001$. We use time series for a sample time of $\Delta t = 1$ for Henon and Ikeda systems, $\Delta t = 0.03$ for the Lorenz system and $\Delta t = 0.12$ for the Rössler system. The time series from $N(0,1)$ and $U(0,1)$ distributions are generated using respectively the routines RNNOF and RNUN of the $IMSL$ (International Mathematical and Statistics Libraries).

TABLE 2

HENON

$N = 50000,\ K = 5000,\ NV = \max\{6, D+4\},\ N_T = 25$

$\lambda_{K,1} = 0.4193$	$\lambda_{K,2} = -1.6233$
$\alpha_1 = 0.4194$	$\alpha_2 = -1.6107$

	$m=2$	$m=3$	$m=4$	$m=5$	$m=6$	$m=7$
$\alpha_1^{(m,2)}$	0.473	0.424	0.419	0.418	0.419	0.419
$\alpha_2^{(m,2)}$	−1.530	−1.571	−1.580	−1.566	−1.580	−1.567
$\alpha_1^{(m,m)}$		0.472	0.768	0.835	0.838	0.868
$\alpha_2^{(m,m)}$		0.343	0.417	0.420	0.419	0.740
$\alpha_3^{(m,m)}$		−1.642	−1.478	−0.863	−0.009	0.400
$\alpha_4^{(m,m)}$			−3.420	−1.882	−1.329	−0.461
$\alpha_5^{(m,m)}$				−6.004	−2.627	−1.192
$\alpha_6^{(m,m)}$					−8.217	−1.890
$\alpha_7^{(m,m)}$						−11.802

Liapunov exponents of the Henon system. At the top of the table appear the estimates using an orbit of the system. The estimates using the tangent map are $\lambda_{K,i}, i = 1, 2$, and the estimates using the best linear fits are α_i, $i = 1, 2$. The results obtained from a scalar time series using the observable $h(x, y) = x^2 + y^2$ appear below and they are denoted by $\alpha_i^{(m,D)}, i = 1, ..., D$. The bottom table for the exponents $\alpha_j^{(m,m)}, j = 1, ..., m$ illustrates the issue of the spurious exponents.

TABLE 3

HENON

$N = 500000,\ K = 15000,\ NV = 10,\ N_T = 25$

$\lambda_{K,1} = 0.4192$	$\lambda_{K,2} = -1.6231$
$\alpha_1 = 0.4191$	$\alpha_2 = -1.6223$

	$m=2$	$m=3$	$m=4$	$m=5$	$m=6$	$m=7$
$\alpha_1^{(m,2)}$	0.4578	0.4199	0.4185	0.4189	0.4191	0.4157
$\alpha_2^{(m,2)}$	−1.5900	−1.6046	−1.6142	−1.6223	−1.6244	−1.6259

$N = 1000,\ K = 990,\ NV = 5,\ N_T = 15$

$\lambda_{K,1} = 0.4336$	$\lambda_{K,2} = -1.6376$
$\alpha_1 = 0.4351$	$\alpha_2 = -1.5684$

	$m=2$	$m=3$	$m=4$	$m=5$	$m=6$	$m=7$
$\alpha_1^{(m,2)}$	0.6176	0.4429	0.4449	0.4347	0.4145	0.4140
$\alpha_2^{(m,2)}$	−1.0834	−1.4770	−1.4161	−1.3133	−1.1886	−1.0351

Liapunov exponents of the Henon system. Results for a long and a short time series taking $D = 2$ as the dimension where the linear fits are performed. In the scalar case we are using the observable $h(x, y) = x^2 + y^2$.

TABLE 4

IKEDA

$N = 500000,\ K = 15000,\ NV = 10,\ N_T = 25$

$\lambda_{K,1} = 0.5110$	$\lambda_{K,2} = -0.7217$
$\alpha_1 = 0.5110$	$\alpha_2 = -0.7221$

	$m=2$	$m=3$	$m=4$	$m=5$	$m=6$	$m=7$
$\alpha_1^{(m,2)}$	1.2843	0.5144	0.5110	0.5112	0.5106	0.5105
$\alpha_2^{(m,2)}$	−0.6262	−0.7234	−0.7217	−0.7219	−0.7215	−0.7210

$N = 1000,\ K = 990,\ NV = 10,\ N_T = 25$

$\lambda_{K,1} = 0.5078$	$\lambda_{K,2} = -0.7185$
$\alpha_1 = 0.4932$	$\alpha_2 = -0.7749$

	$m=2$	$m=3$	$m=4$	$m=5$	$m=6$	$m=7$
$\alpha_1^{(m,2)}$	0.7529	0.4984	0.4849	0.4744	0.4455	0.3994
$\alpha_2^{(m,2)}$	−0.5941	−0.7706	−0.7242	−0.7132	−0.6934	−0.6092

Liapunov exponents of the Ikeda system. Results for a long and a short time series. The scalar time series is obtained using the observable $h(x, y) = \ln(1 + x^2 + y^2)$.

TABLE 5

LORENZ $N = 100000$, $K = 10000$, $NV = \max\{6, D+2\}$, $N_T = 25$						
$\alpha_1 = 1.495$, $\alpha_2 = 0.027$, $\alpha_3 = -19.894$						
	$m = 3$	$m = 4$	$m = 5$	$m = 6$	$m = 7$	$m = 8$
$\alpha_1^{(m,3)}$	4.294	1.878	1.603	1.526	1.537	1.504
$\alpha_2^{(m,3)}$	−0.966	−0.184	−0.031	−0.011	−0.032	−0.016
$\alpha_3^{(m,3)}$	−23.730	−23.314	−23.033	−22.750	−22.010	−21.071
$\alpha_1^{(m,m)}$		1.515	2.256	3.529	4.406	4.579
$\alpha_2^{(m,m)}$		0.024	1.057	1.478	1.553	1.712
$\alpha_3^{(m,m)}$		−6.458	−0.294	0.186	1.124	1.298
$\alpha_4^{(m,m)}$		−22.727	−5.799	−0.932	−0.124	0.013
$\alpha_5^{(m,m)}$			−28.803	−10.250	−3.230	−1.242
$\alpha_6^{(m,m)}$				−39.894	−18.494	−8.155
$\alpha_7^{(m,m)}$					−66.339	−22.025
$\alpha_8^{(m,m)}$						−99.154

Liapunov exponents of the Lorenz dynamics. The scalar time series is obtained using the observable $h(x, y, z) = z$. Study of the dependence of the estimates on m and D.

TABLE 6

$LORENZ$, $u_i = y_i$

$N = 100000$, $K = 10000$, $NV = 6$, $N_T = 25$

	$m=2$	$m=3$	$m=4$	$m=5$	$m=6$	$m=7$	$m=8$
$\alpha_1^{(m,2)}$	25.3697	7.0058	4.7285	2.7706	2.2330	1.8587	1.6733
$\alpha_2^{(m,2)}$	−5.1752	−5.3109	−3.4121	−1.9610	−1.2353	−0.7798	−0.4810

	$m=9$	$m=10$	$m=11$	$m=12$	$m=13$	$m=14$	$m=15$
$\alpha_1^{(m,2)}$	1.5757	1.5968	1.5457	1.5074	1.4688	1.5490	1.4770
$\alpha_2^{(m,2)}$	−0.3888	−0.3486	−0.2178	−0.1691	−0.1099	−0.1959	−0.1041

Results for a scalar time series from the Lorenz system taking $D = 2$ as the dimension where the linear fits are performed.

TABLE 7

LORENZ
$N = 500000$, $K = 10000$, $NV = 10$, $N_T = 25$
$\alpha_{K,N,1} = 1.4979$, $\alpha_{K,N,2} = 0.0158$, $\alpha_{K,N,3} = -20.0226$

	$m=3$	$m=4$	$m=5$	$m=6$	$m=7$	$m=8$
$\alpha_1^{(m,3)}$	3.7285	1.5453	1.5121	1.5233	1.5117	1.5010
$\alpha_2^{(m,3)}$	−0.6885	−0.0604	0.0013	−0.0192	−0.0094	0.0012
$\alpha_3^{(m,3)}$	−25.3491	−25.5362	−24.6822	−23.8908	−22.6678	−22.4483

$N = 5000$, $K = 4990$, $NV = 6$, $N_T = 15$
$\alpha_{K,N,1} = 1.4804$, $\alpha_{K,N,2} = 0.0396$, $\alpha_{K,N,3} = -22.2711$

	$m=3$	$m=4$	$m=5$	$m=6$	$m=7$	$m=8$	$m=9$
$\alpha_1^{(m,3)}$	4.875	3.676	2.748	2.0412	1.729	1.582	1.506
$\alpha_2^{(m,3)}$	−1.609	−1.362	−0.885	−0.426	−0.204	−0.179	−0.004
$\alpha_3^{(m,3)}$	−22.233	−21.985	−20.378	−19.648	−18.293	−17.798	−17.001

Liapunov exponents for the Lorenz system. The scalar time series is obtained using the observable $h(x, y, z) = y$. The top table shows the results for a long time series taking $D = 3$. The bottom table shows the results for $N = 5000$ which is the shortest lenght giving addequate estimates of the positive exponent.

TABLE 8

RÖSSLER						
$N = 500000$, $K = 25000$, $NV = 10$, $N_T = 25$						
$\alpha_{K,N,1} = 0.0761$, $\alpha_{K,N,2} = -0.0010$, $\alpha_{K,N,3} = -5.7165$						
	$m = 3$	$m = 4$	$m = 5$	$m = 6$	$m = 7$	$m = 8$
$\alpha_1^{(m,3)}$	0.0831	0.0731	0.0649	0.0686	0.0660	0.0680
$\alpha_2^{(m,3)}$	0.0014	−0.0111	−0.0126	−0.0036	0.0111	0.0003
$\alpha_3^{(m,3)}$	−4.5435	−4.8756	−5.1958	−5.2634	−5.2570	−5.0962

$N = 5000$, $K = 4990$, $NV = 6$, $N_T = 15$								
$\alpha_{K,N,1} = 0.0646$, $\alpha_{K,N,2} = 0.0045$, $\alpha_{K,N,3} = -0.7920$								
	$m = 3$	$m = 4$	$m = 5$	$m = 6$	$m = 7$	$m = 8$	$m = 9$	$m = 10$
$\alpha_1^{(m,3)}$	0.2419	0.1616	0.1230	0.109	0.009	0.079	0.077	0.067
$\alpha_2^{(m,3)}$	0.0196	−0.0125	−0.0060	−0.0001	−0.007	−0.009	−0.009	0.004
$\alpha_3^{(m,3)}$	−16.192	−2.6366	−2.7545	−2.332	−2.367	−2.162	−1.999	−1.820

Liapunov exponents of the Rössler system. The scalar time series is obtained using the observable $h(x, y, z) = x + y + z$. At the top of the table appear the results for a long time series. At the bottom appear the results using a lenght $N = 5000$.

TABLE 9

HENON, $K = 1000$, $h(x, y) = x$				
N	Z_B	NV	$\lambda_1^{(6,2)}$	$\lambda_2^{(6,2)}$
50000	0	6	0.422	−1.604
100000	0	6	0.338	−3.911
250000	0	6	0.329	−4.223
250000	0.001	73	0.424	−1.669
250000	0.0001	41	0.423	−1.663
250000	0.00001	27	0.423	−1.633

Lipaunov exponents of the Henon system. Results for a long scalar time series recorded with only seven digits of precision. When $Z_B > 0$, NV is the average number of neigbouring points used in performing the linear fits.

- *FIG* 1. Results of the dimension algorithm for a time series of Ikeda system with the observable $h(x,y) = \ln(1+x^2+y^2)$. Entry parameters values $N = 50000$, $r_{\max} = 0.05$, $m_{\max} = 10$ and $K = 2500$.
  - (a) $\overline{\mathrm{VAR}}_{K,N,m,r,j}$; $m = 2, ..., 10$; $j = 1, ..., m$.
  - (b) $\overline{\mathrm{VAR}}_{K,N,m,r_i,3}$; $m = 3, ..., 10$.

- *FIG* 2. Results of the dimension algorithm for time series from an Uniform in the interval $[0,1]$ distribution. Entry parameters $N = 50000$, $m_{\max} = 10$, $r_{\max} = 0.1$, and $K = 1000$.

- *FIG* 3. Results of the dimension algorithm for a short lenght time series from Henon system with the observable $h(x,y) = x^2 + y^2$. Entry parameters $N = 5000$, $r_{\max} = 0.2$, $m_{\max} = 10$ and $K = 2500$.
  - (a) $\overline{\mathrm{VAR}}_{K,N,m,r,j}$; $m = 2, ..., 10$; $j = 1, ..., m$.
  - (b) $\overline{\mathrm{VAR}}_{K,N,m,r,3}$; $m = 3, ..., 10$.

- *FIG* 4. Results of the dimension algorithm for the Lorenz dynamics obtained from an orbit of the system (a), and scalar time series using the observable $h(x,y,z) = y$ in (b) to (e). Entry parameters for figures (a) to (c) : $N = 50000$, $r_{\max} = 0.05$, $m_{\max} = 10$ and $K = 2500$. In (d) the entry parameters are $N = 500000$, $r_{\min} = 0.0025$, $r_{\max} = 0.03$, $K = 2500$ and $N_{\min} = 25$. The averages are made with 129 data points from the $K = 2500$ avalaible points.
  - (a) $\overline{\mathrm{VAR}}_{K,N,r,j}$; $j = 1, ..., 3$.
  - (b) $\overline{\mathrm{VAR}}_{K,N,m,r,j}$; $m = 2, ..., 10$; $j = 1, ..., m$.
  - (c) $\overline{\mathrm{VAR}}_{K,N,m,r,3}$; $m = 3, ..., 10$.
  - (d) $\mathrm{LNVAR}_{K,N,m,r}(3)$, $m = 7, ..., 10$.

- *FIG* 5. Results of the dimension algorithms for the Rössler dynamics obtained from an orbit of the system (a), and scalar time series using the observable $h(x,y,z) = z$ in (b) to (e). Entry parameters for figures (a) to (c) : $N = 50000$, $r_{\max} = 0.05$, $m_{\max} = 10$ and $K = 2500$. In (d) the entry parameters are $N = 500000$, $r_{\min} = 0.00175$, $r_{\max} = 0.05$, $K = 2500$ and $N_{\min} = 35$. The averages are made with 160 data points from the $K = 2500$ avalaible points.
  - (a) $\overline{\mathrm{VAR}}_{K,N,r,j}$; $j = 1, ..., 3$.

(b) $\overline{\mathrm{VAR}}_{K,N,m,r,j}$; $m = 2, ..., 10$; $j = 1, ..., m$.
(c) $\overline{\mathrm{VAR}}_{K,N,m,r,3}$; $m = 3, ..., 10$.
(d) $\mathrm{LNVAR}_{K,N,m,r}(3)$, $m = 7, ..., 10$.

- *FIG* 6. Results of the smoothness parameter for the Lorenz dynamics using an orbit of the dynamics (*a*) and a scalar time series with the observable $h(x, y, z) = y$ in (*b*) to (*e*). Entry parameters a exception of the (*d*) figure: $N = 50000$, $r_{\max} = 0.05$, $N_{\mathrm{T}} = 25$ and $K = 1000$.
  (a) Results from an orbit of the dynamics.
  (b) Results for a scalar time series for $m \in \{3, 4, 5, 6\}$ and $d = 3$.
  (c) Results for a scalar time series for $m \in \{7, 8\}$ and $d = 3$.
  (d) Results for a short length scalar time series. Entry parameters: $N = 1000$, $r_{\max} = 0.2$, $N_{\mathrm{T}} = 15$, $K = 900$, $m \in \{7, 8\}$ and $d = 3$.
  (e) Results for a scalar time series for $m = d = 1$.
  (f) Results for a scalar time series for $m = 7$ and $d \in \{1, 2, 3, 4, 5\}$

- *FIG* 6. Results of the smoothness parameter for an orbit and a scalar time series from the Henon map using the observable $h(x, y) = x^2 + y^2$. Entry parameters: $N = 50000$, $r_{\max} = 0.05$, $N_{\mathrm{T}} = 25$ and $K = 1000$.
  (a) Results from an orbit.
  (b) Results for a scalar time series for $m \in \{2, 3, 4, 5, 6, 7\}$ and $d = 2$.

- *Fig.* 7. Results of the smoothness parameter for a scalar time series of points from the $N(0, 1)$ distribution for $m = d \in \{1, 2, 3\}$. Entry parameters $N = 50000$, $r_{\max} = 0.05$, $N_{\mathrm{T}} = 25$ and $K = 1000$.

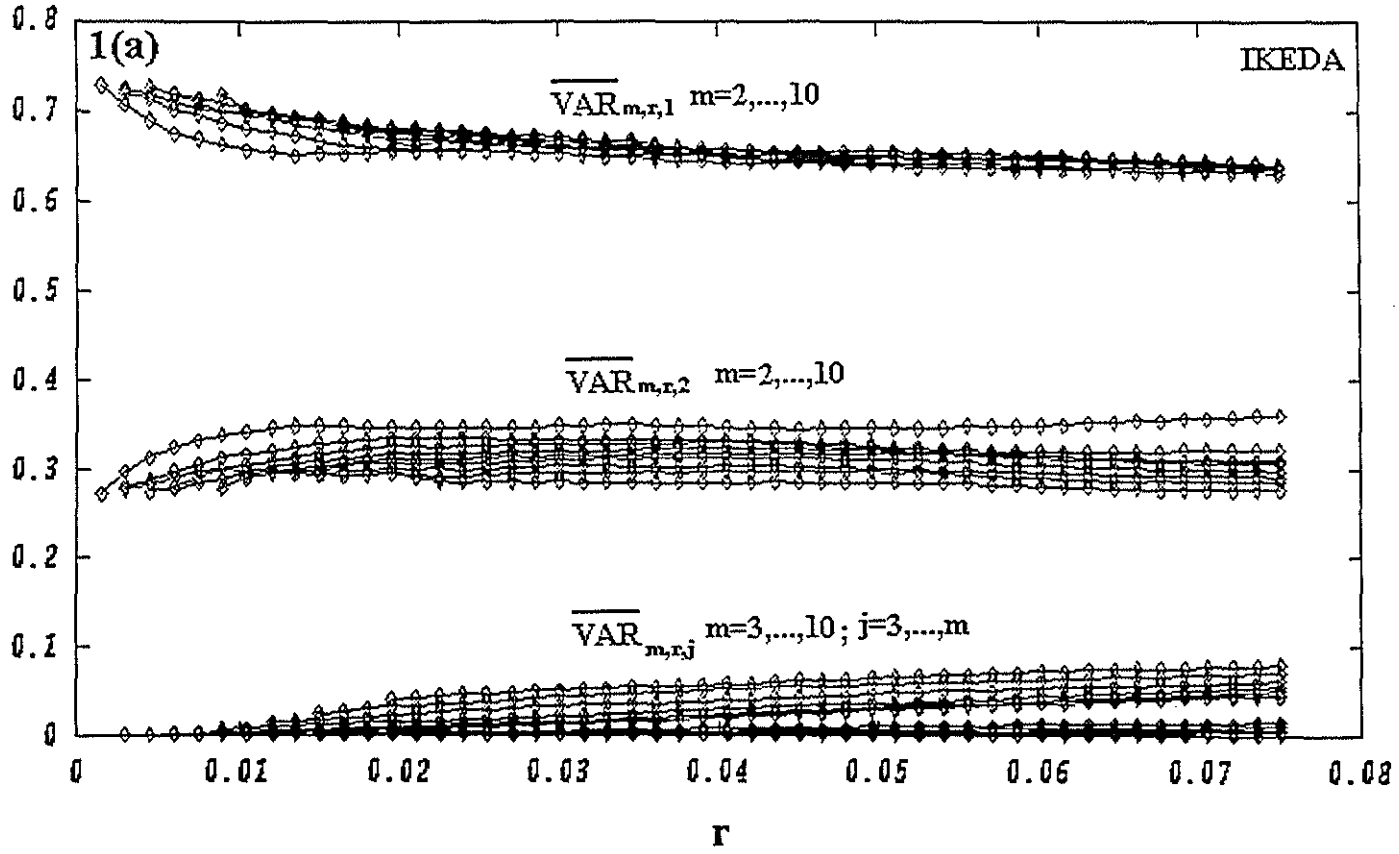
1(a)
IKEDA
$\overline{VAR}_{m,r,1}$ m=2,...,10
$\overline{VAR}_{m,r,2}$ m=2,...,10
$\overline{VAR}_{m,r,j}$ m=3,...,10 ; j=3,...,m
0.8
0.7
0.6
0.5
0.4
0.3
0.2
0.1
0
0
0.01
0.02
0.03
0.04
0.05
0.06
0.07
0.08
r

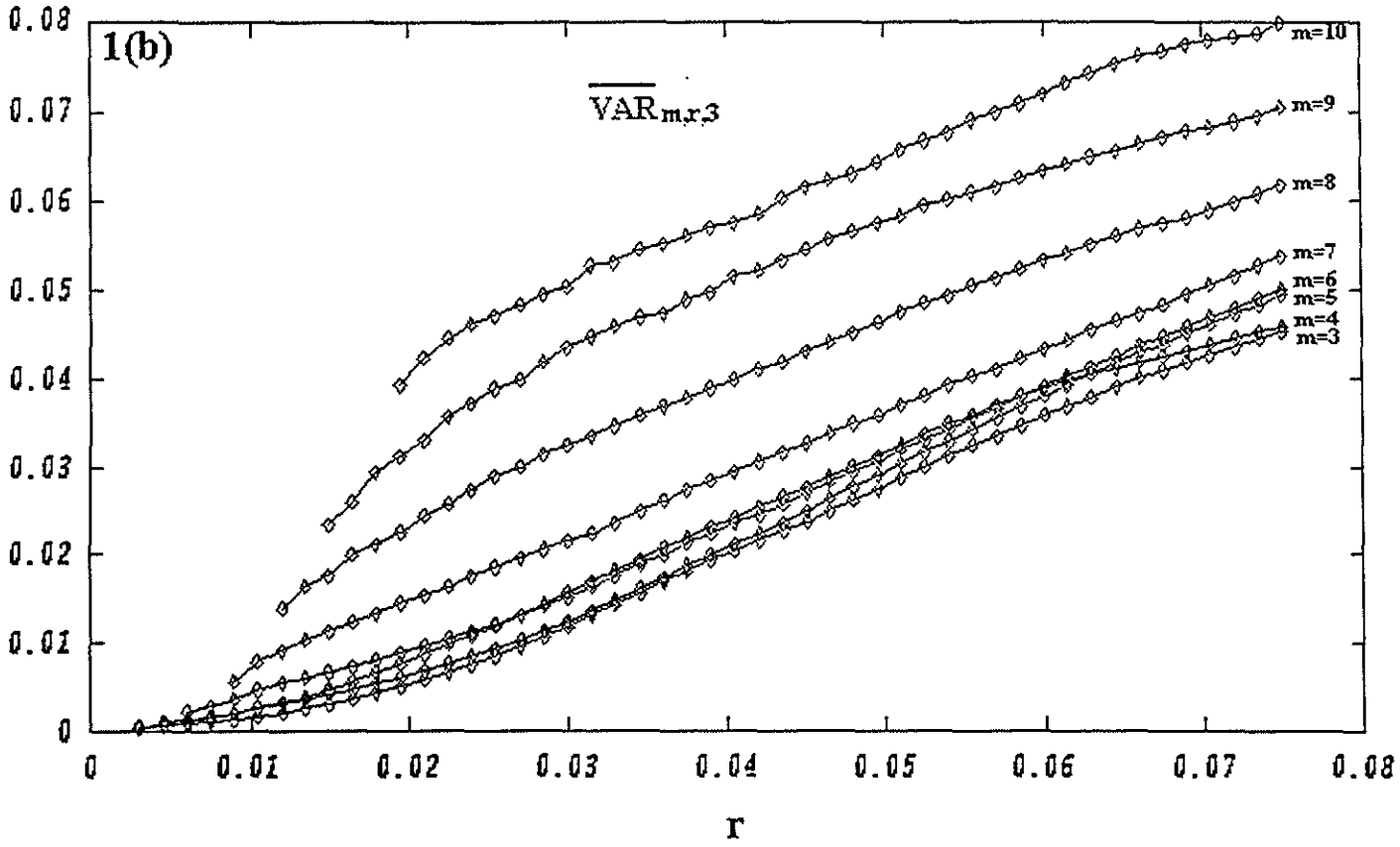
1(b)
$\overline{VAR}_{m,r,3}$
m=10
m=9
m=8
m=7
m=6
m=5
m=4
m=3
0.08
0.07
0.06
0.05
0.04
0.03
0.02
0.01
0
0
0.01
0.02
0.03
0.04
0.05
0.06
0.07
0.08
r

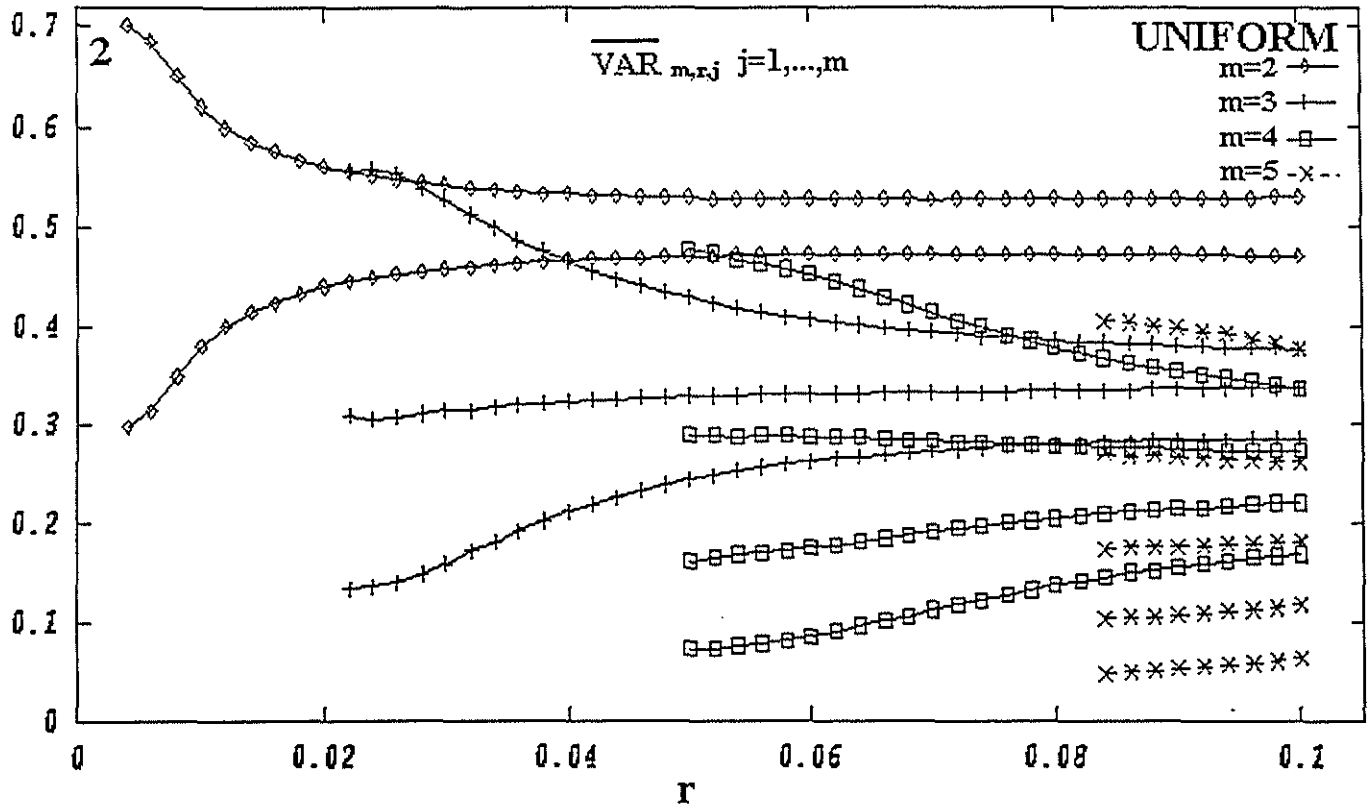
2
$\overline{VAR}_{m,r,j}$ j=1,...,m
UNIFORM
m=2
m=3
m=4
m=5
0.7
0.6
0.5
0.4
0.3
0.2
0.1
0
0
0.02
0.04
0.06
0.08
0.1
r

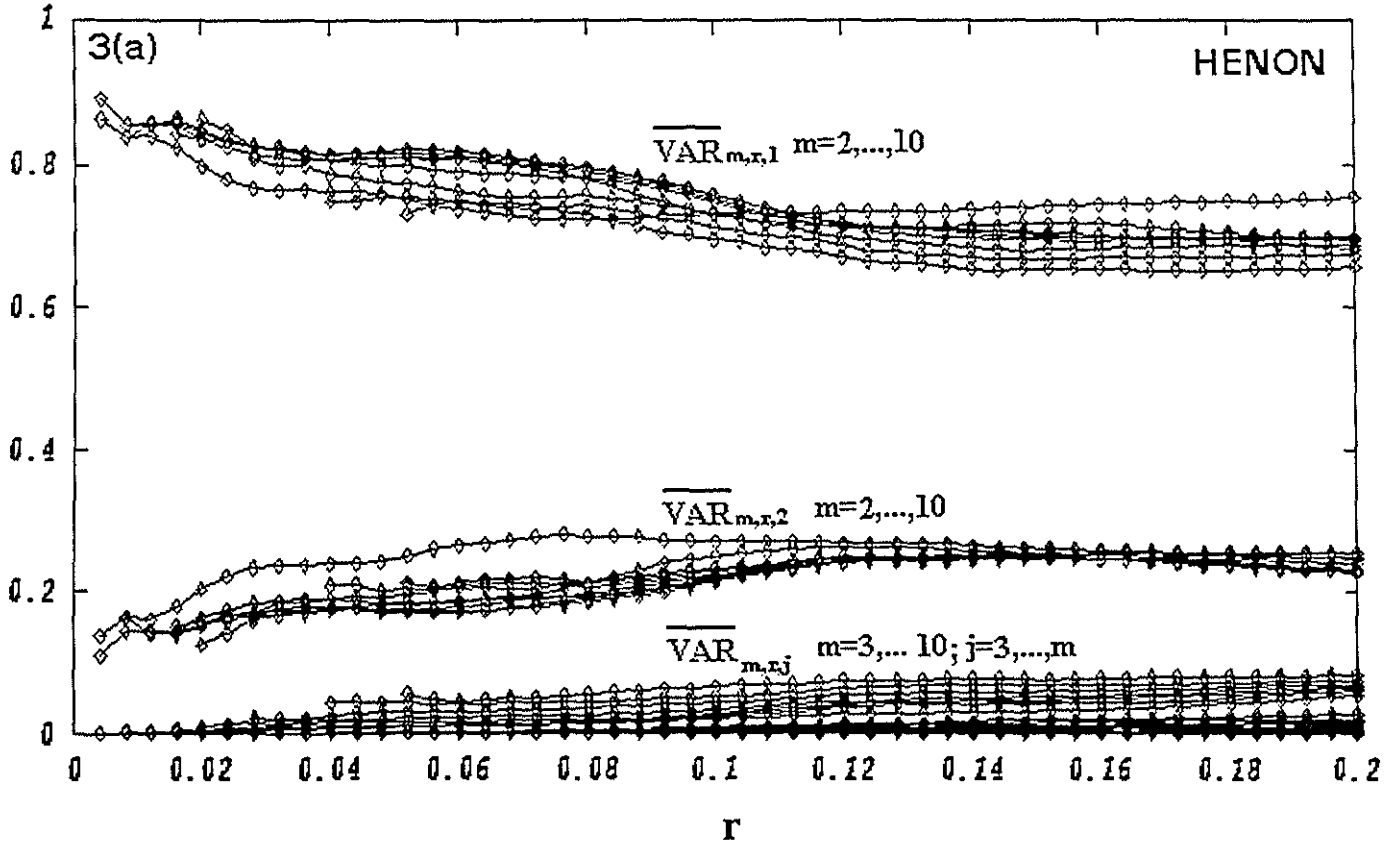
3(a)
HENON
$\overline{VAR}_{m,r,1}$ m=2,...,10
$\overline{VAR}_{m,r,2}$ m=2,...,10
$\overline{VAR}_{m,r,j}$ m=3,... 10; j=3,...,m
1
0.8
0.6
0.4
0.2
0
0
0.02
0.04
0.06
0.08
0.1
0.12
0.14
0.16
0.18
0.2
r

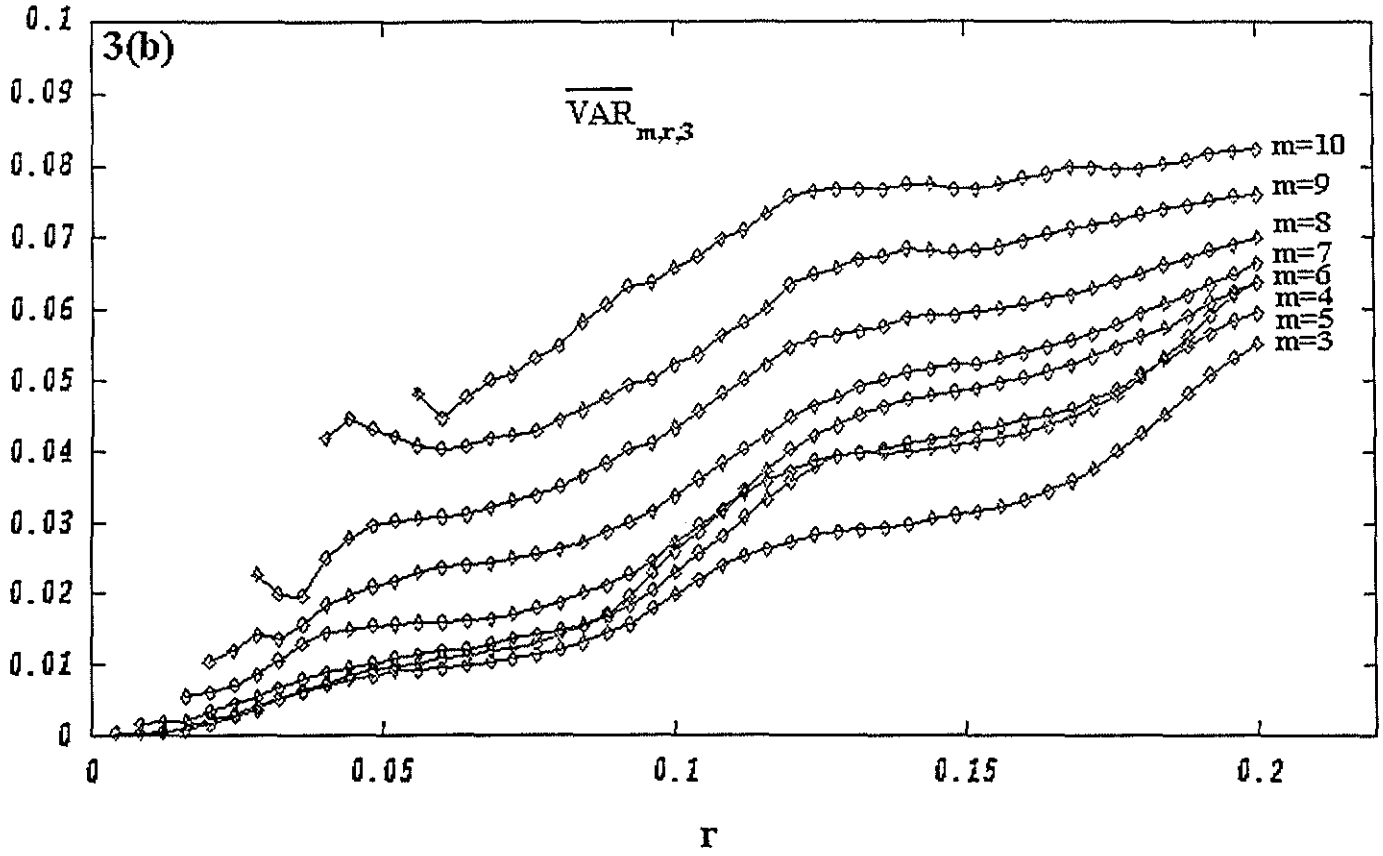
3(b)
$\overline{VAR}_{m,r,3}$
m=10
m=9
m=8
m=7
m=6
m=4
m=5
m=3
0.1
0.09
0.08
0.07
0.06
0.05
0.04
0.03
0.02
0.01
0
0
0.05
0.1
0.15
0.2
r

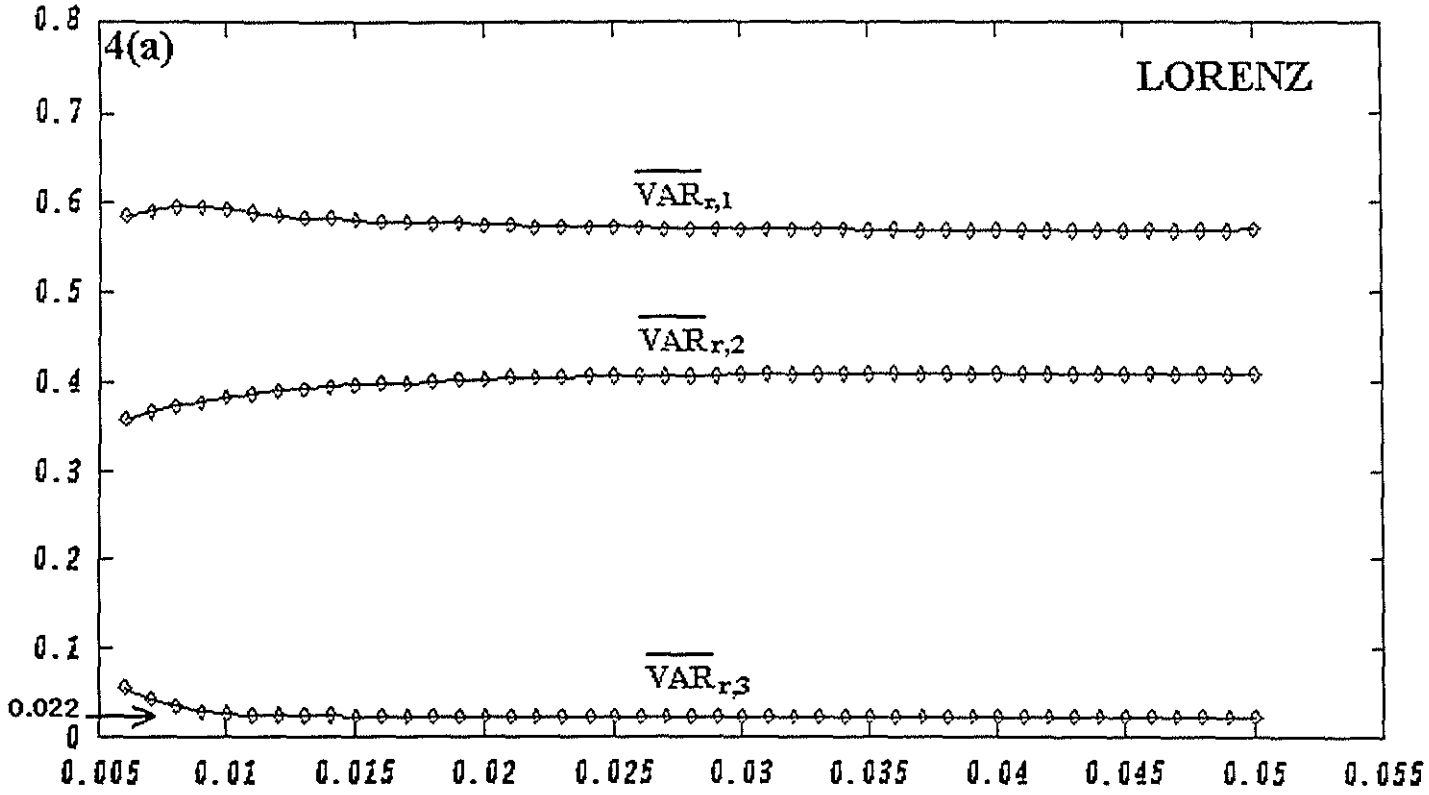
4(a)
LORENZ
$\overline{VAR}_{r,1}$
$\overline{VAR}_{r,2}$
$\overline{VAR}_{r,3}$
0.8
0.7
0.6
0.5
0.4
0.3
0.2
0.1
0.022
0
0.005
0.01
0.015
0.02
0.025
0.03
0.035
0.04
0.045
0.05
0.055

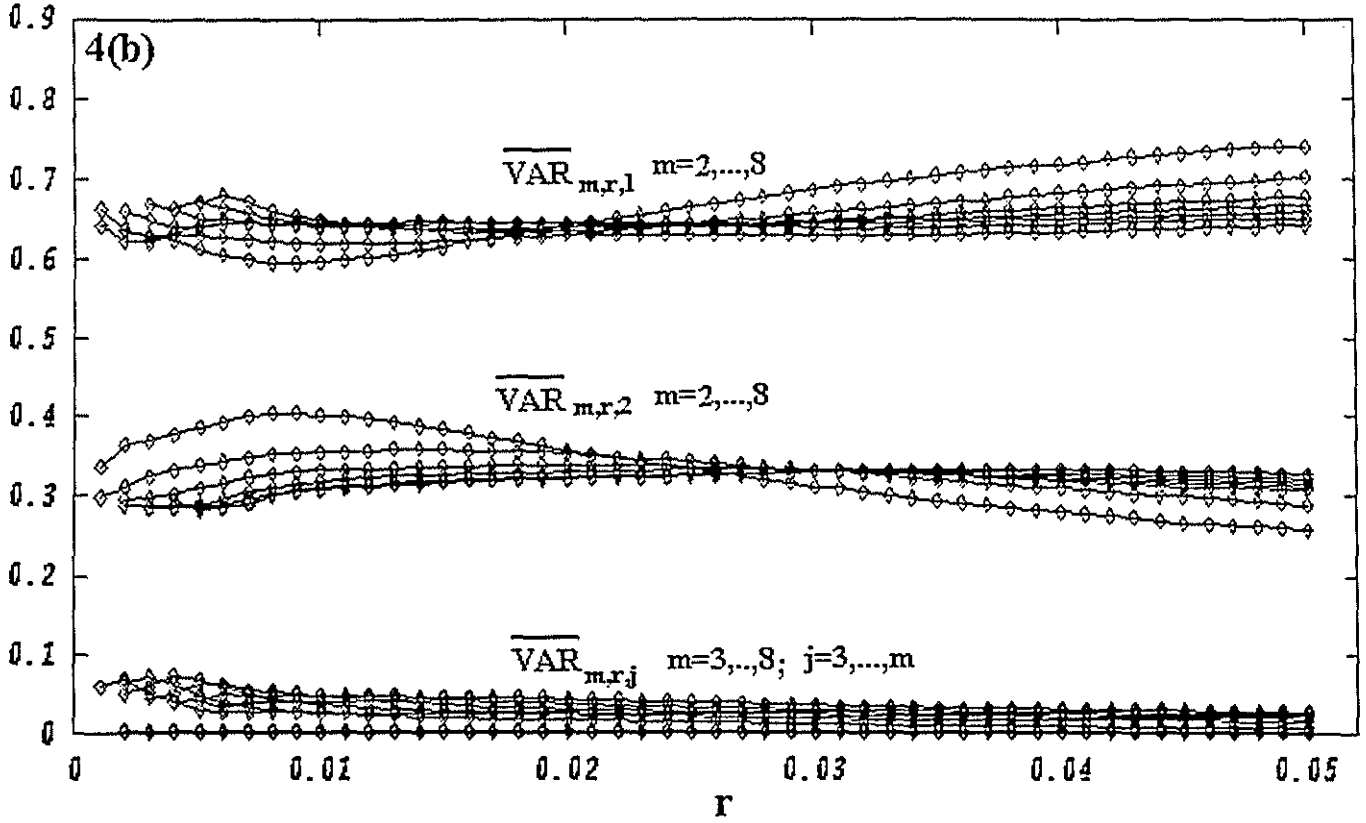
4(b)
$\overline{VAR}_{m,r,1}$ m=2,...,8
$\overline{VAR}_{m,r,2}$ m=2,...,8
$\overline{VAR}_{m,r,j}$ m=3,..,8; j=3,...,m
0.9
0.8
0.7
0.6
0.5
0.4
0.3
0.2
0.1
0
0
0.01
0.02
0.03
0.04
0.05
r

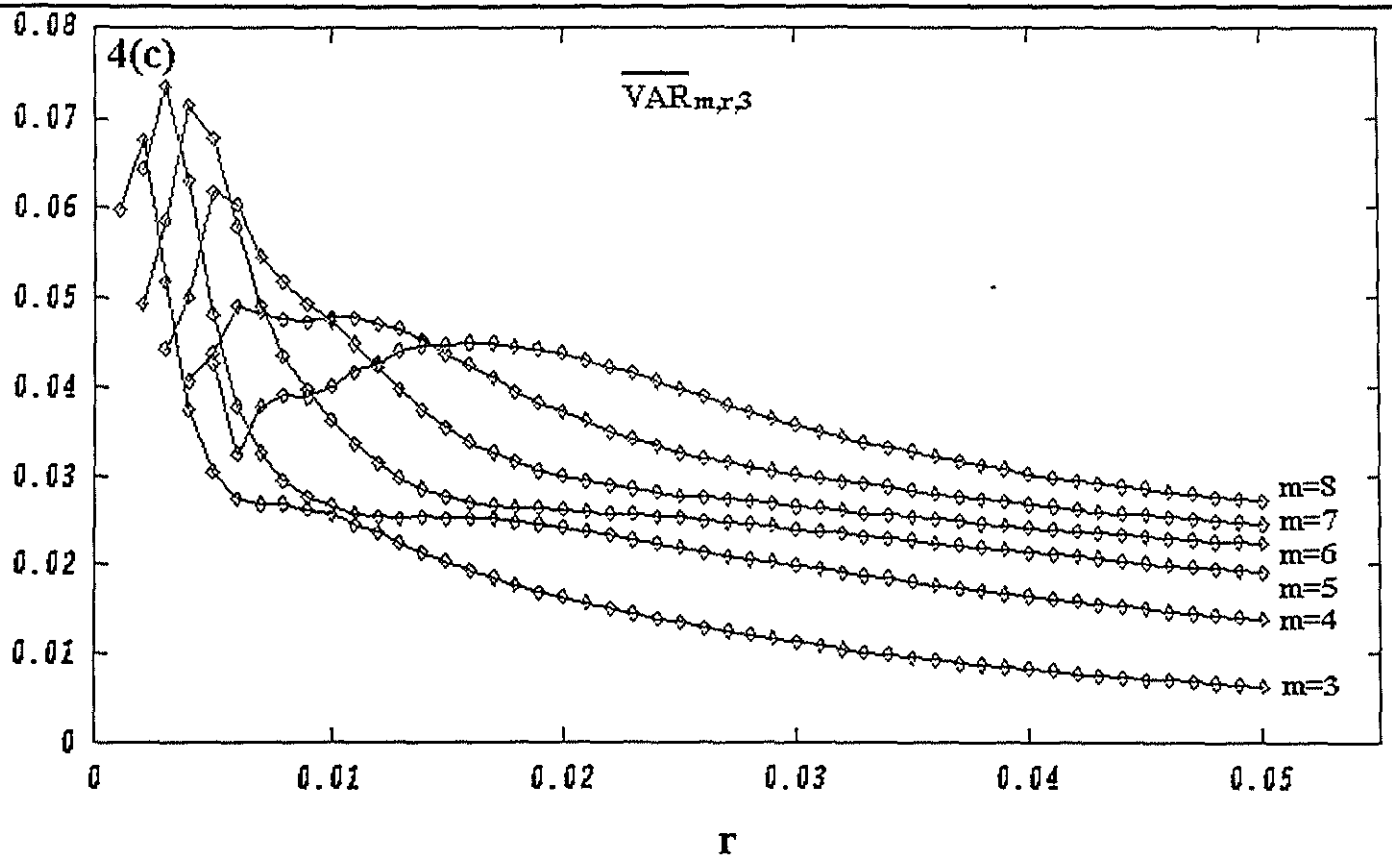
4(c)
$\overline{VAR}_{m,r,3}$
0.08
0.07
0.06
0.05
0.04
0.03
0.02
0.01
0
0
0.01
0.02
0.03
0.04
0.05
m=8
m=7
m=6
m=5
m=4
m=3
r

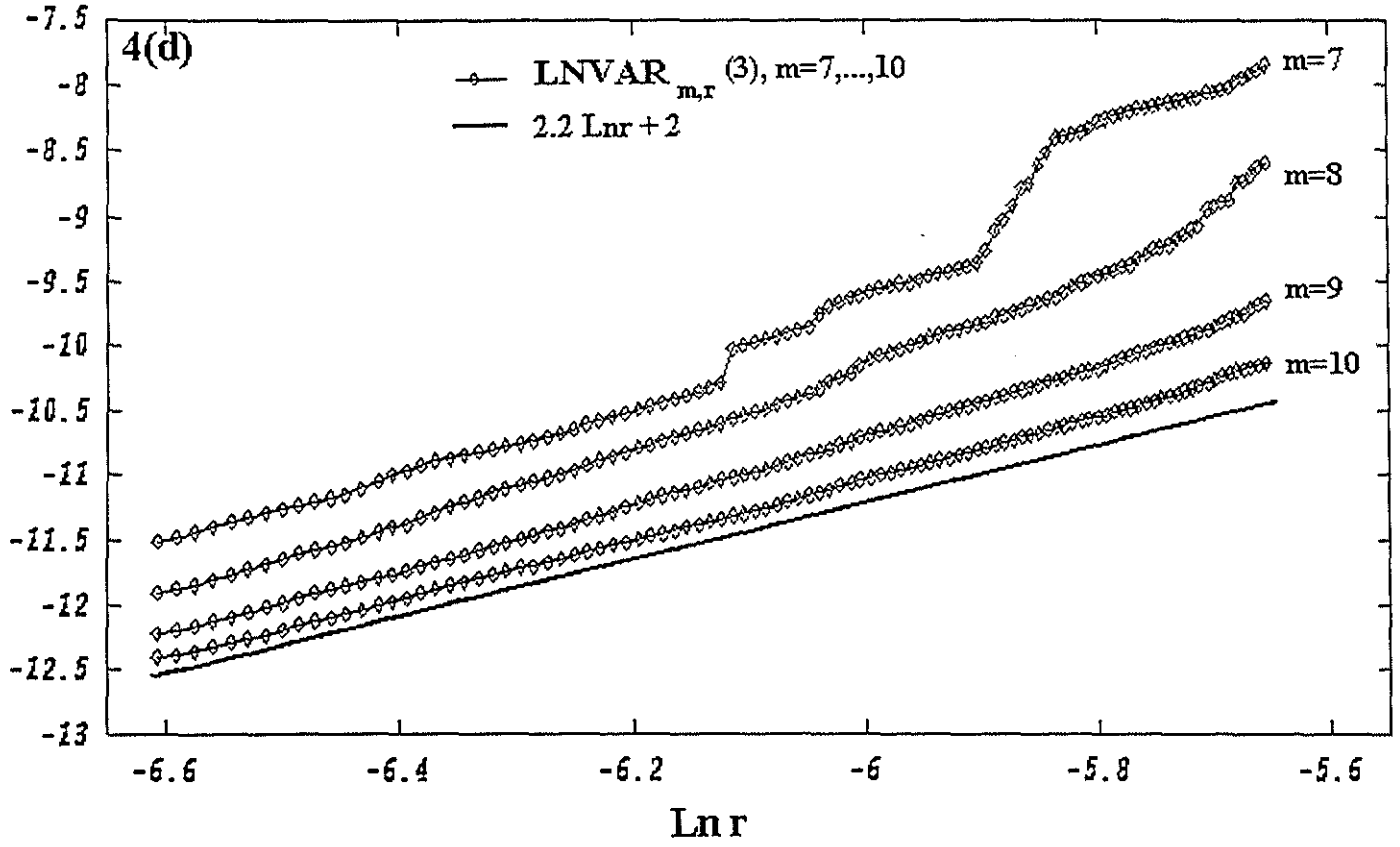
4(d)
LNVAR m,r (3), m=7,...,10
2.2 Lnr + 2
m=7
m=8
m=9
m=10
-7.5
-8
-8.5
-9
-9.5
-10
-10.5
-11
-11.5
-12
-12.5
-13
-6.6
-6.4
-6.2
-6
-5.8
-5.6
Ln r

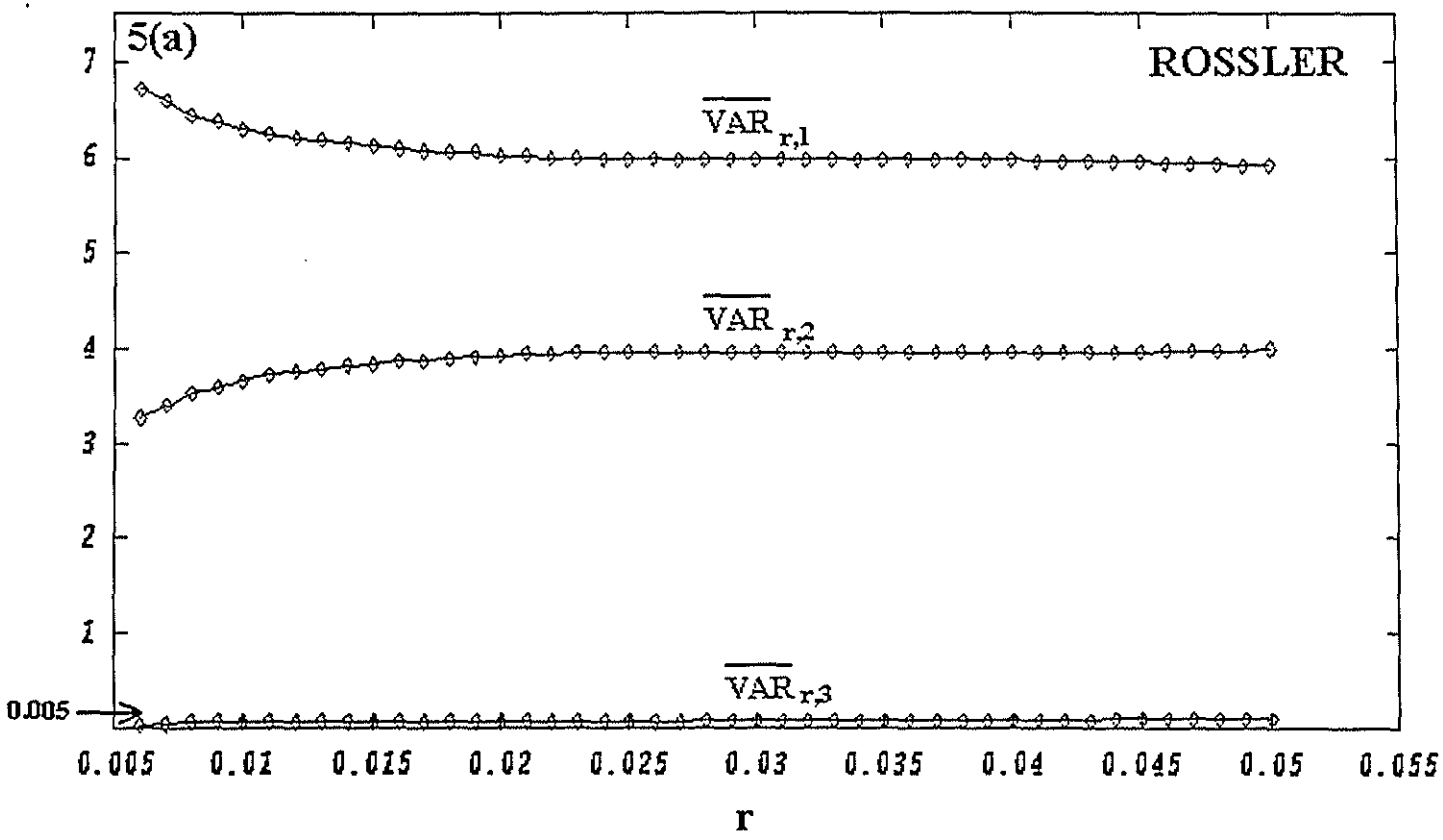
5(a)
ROSSLER
$\overline{VAR}_{r,1}$
$\overline{VAR}_{r,2}$
$\overline{VAR}_{r,3}$
0.005
7
6
5
4
3
2
1
0.005
0.01
0.015
0.02
0.025
0.03
0.035
0.04
0.045
0.05
0.055
r

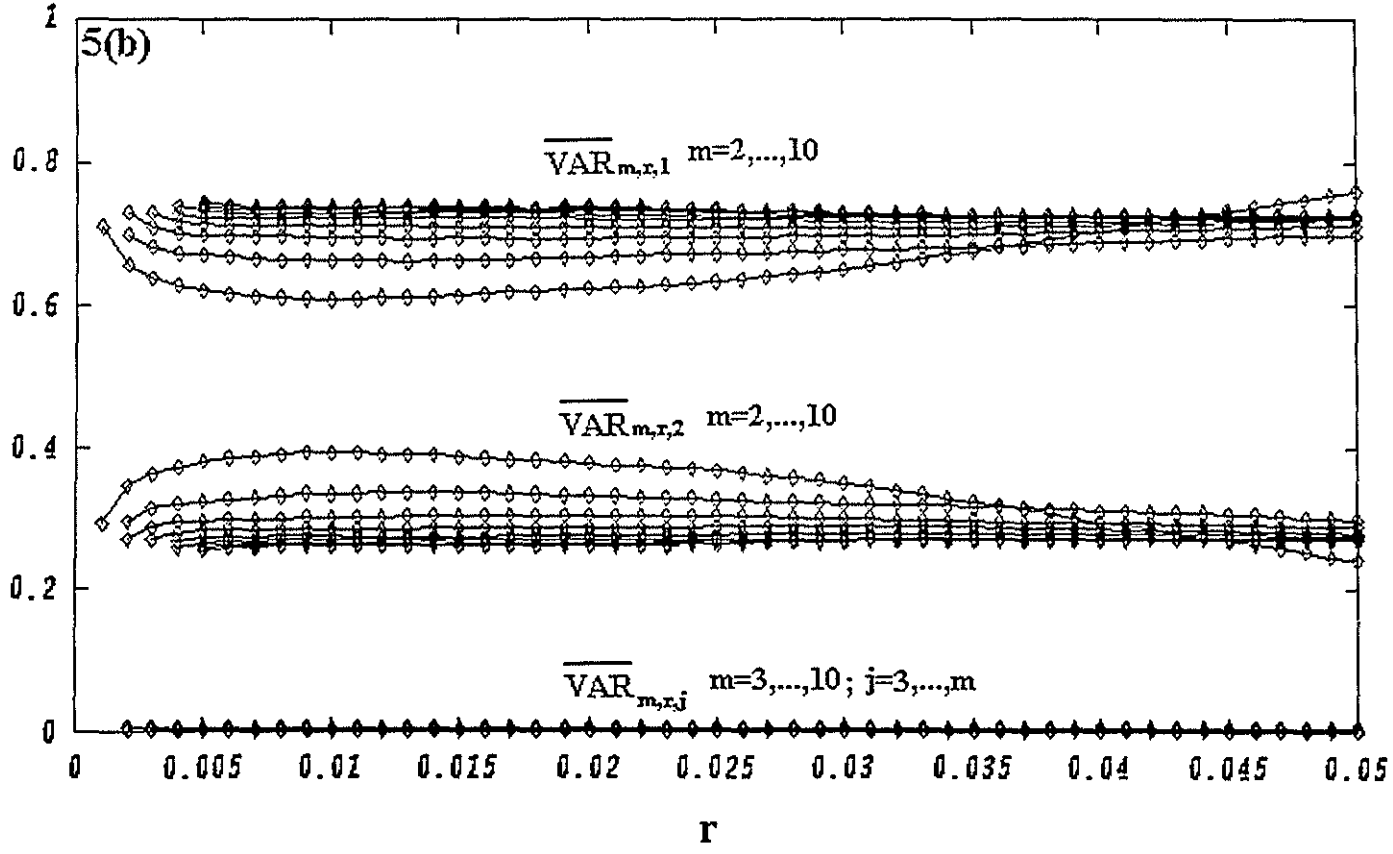
5(b)
$\overline{VAR}_{m,r,1}$ m=2,...,10
$\overline{VAR}_{m,r,2}$ m=2,...,10
$\overline{VAR}_{m,r,j}$ m=3,...,10; j=3,...,m
1
0.8
0.6
0.4
0.2
0
0
0.005
0.01
0.015
0.02
0.025
0.03
0.035
0.04
0.045
0.05
r

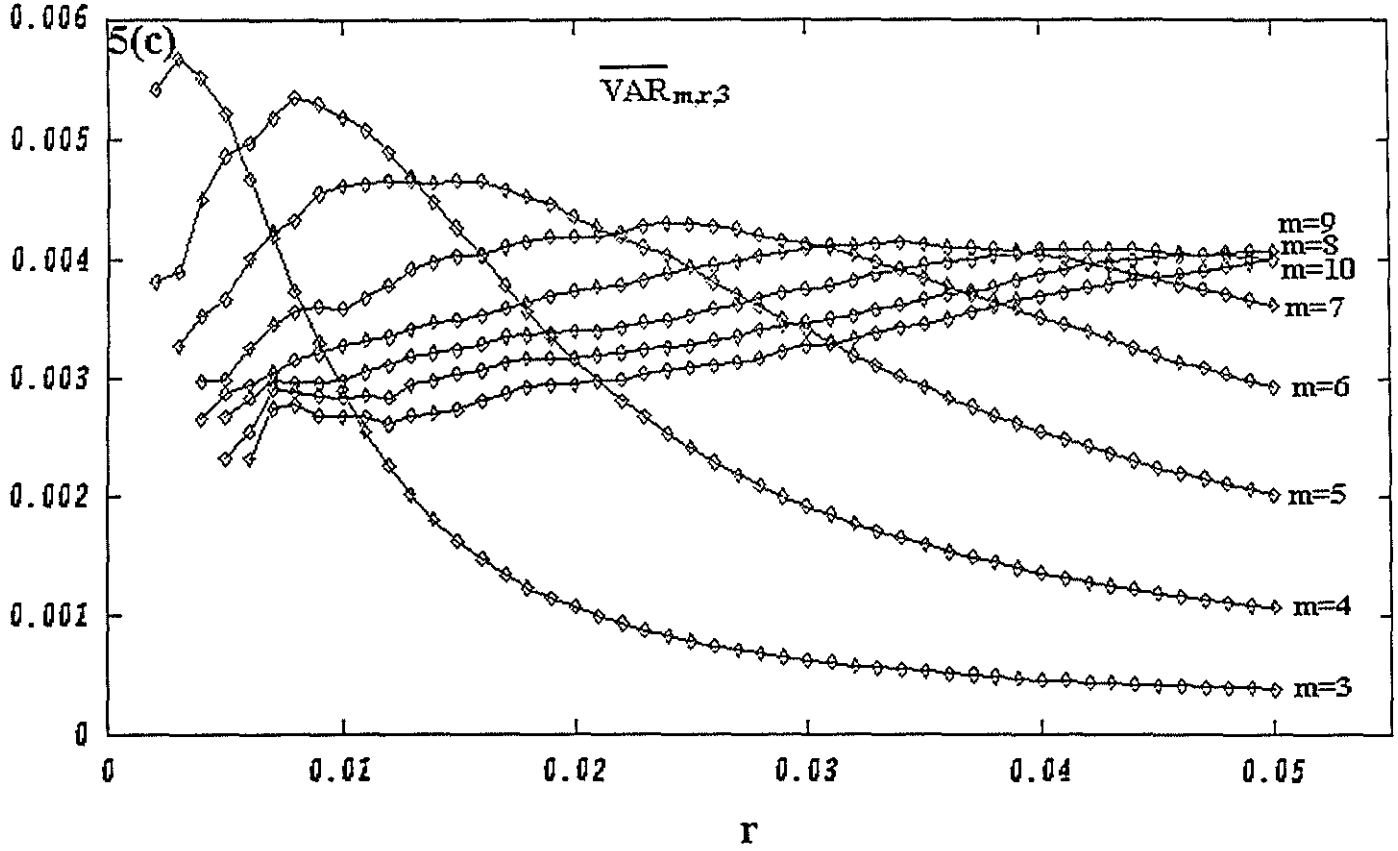
5(c)
$\overline{VAR}_{m,r,3}$
0.006
0.005
0.004
0.003
0.002
0.001
0
0
0.01
0.02
0.03
0.04
0.05
r
m=9
m=8
m=10
m=7
m=6
m=5
m=4
m=3

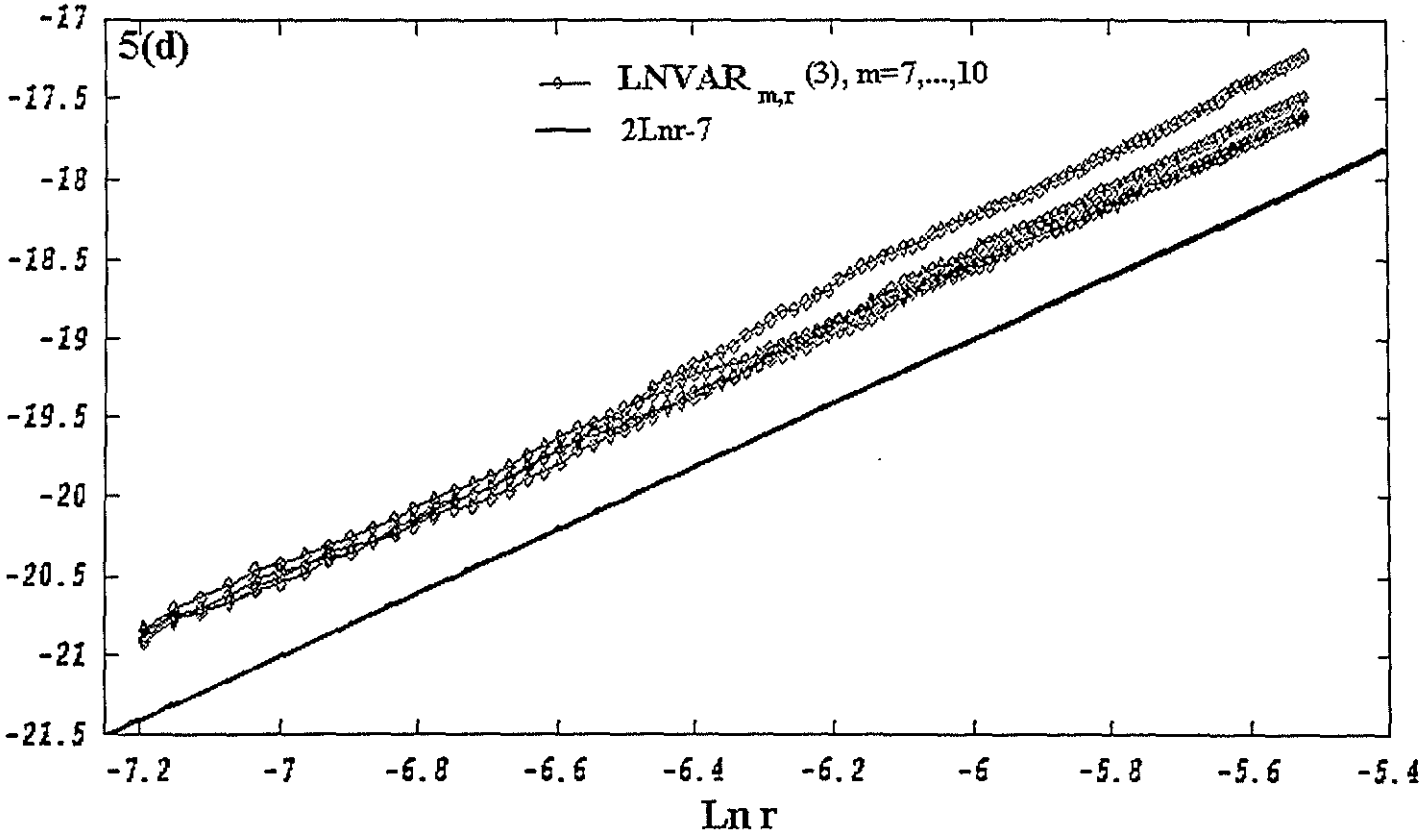
5(d)
LNVAR m,r (3), m=7,...,10
2Lnr-7
-17
-17.5
-18
-18.5
-19
-19.5
-20
-20.5
-21
-21.5
-7.2
-7
-6.8
-6.6
-6.4
-6.2
-6
-5.8
-5.6
-5.4
Ln r

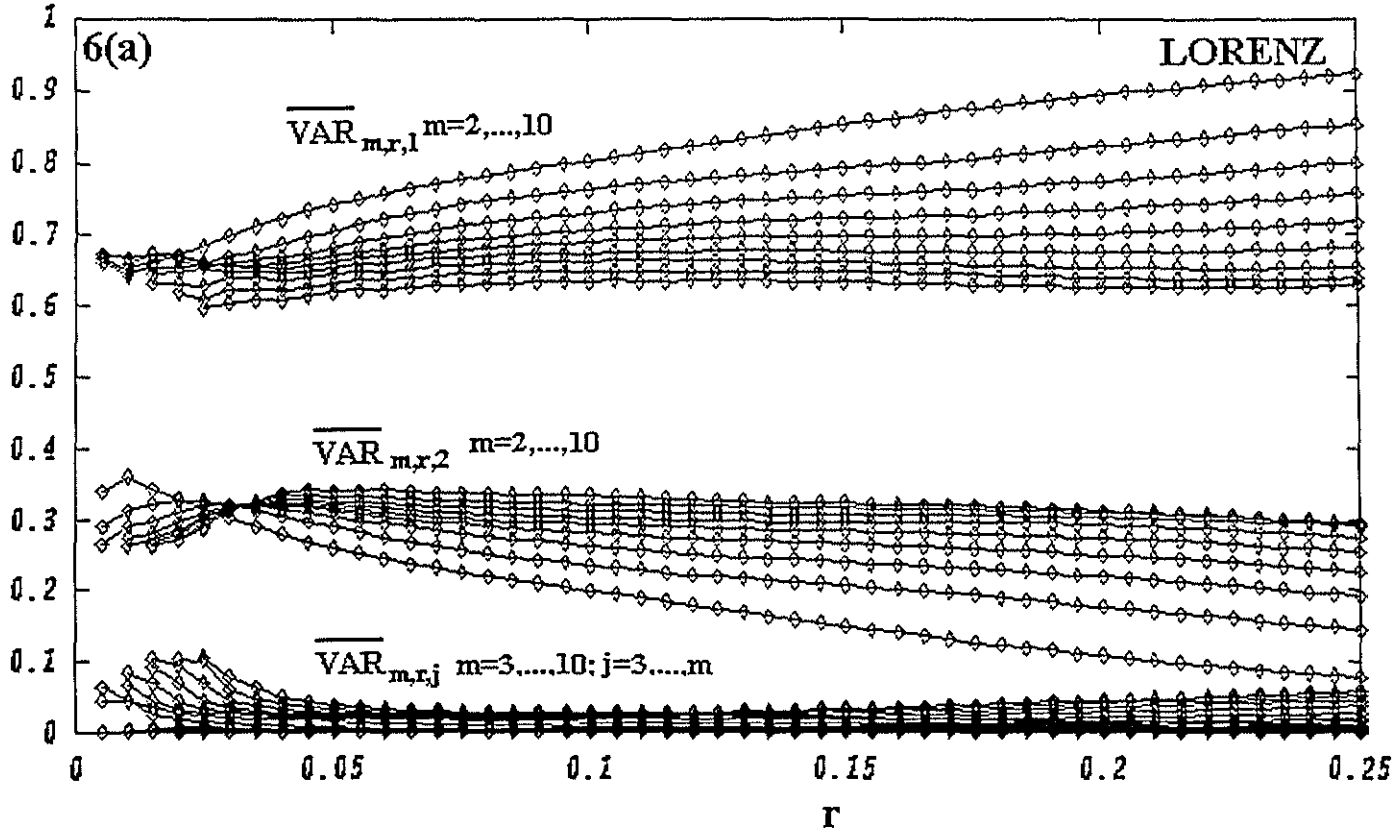
6(a)
LORENZ
$\overline{VAR}_{m,r,1}$ m=2,...,10
$\overline{VAR}_{m,r,2}$ m=2,...,10
$\overline{VAR}_{m,r,j}$ m=3,....,10; j=3,....,m
1
0.9
0.8
0.7
0.6
0.5
0.4
0.3
0.2
0.1
0
0
0.05
0.1
0.15
0.2
0.25
r

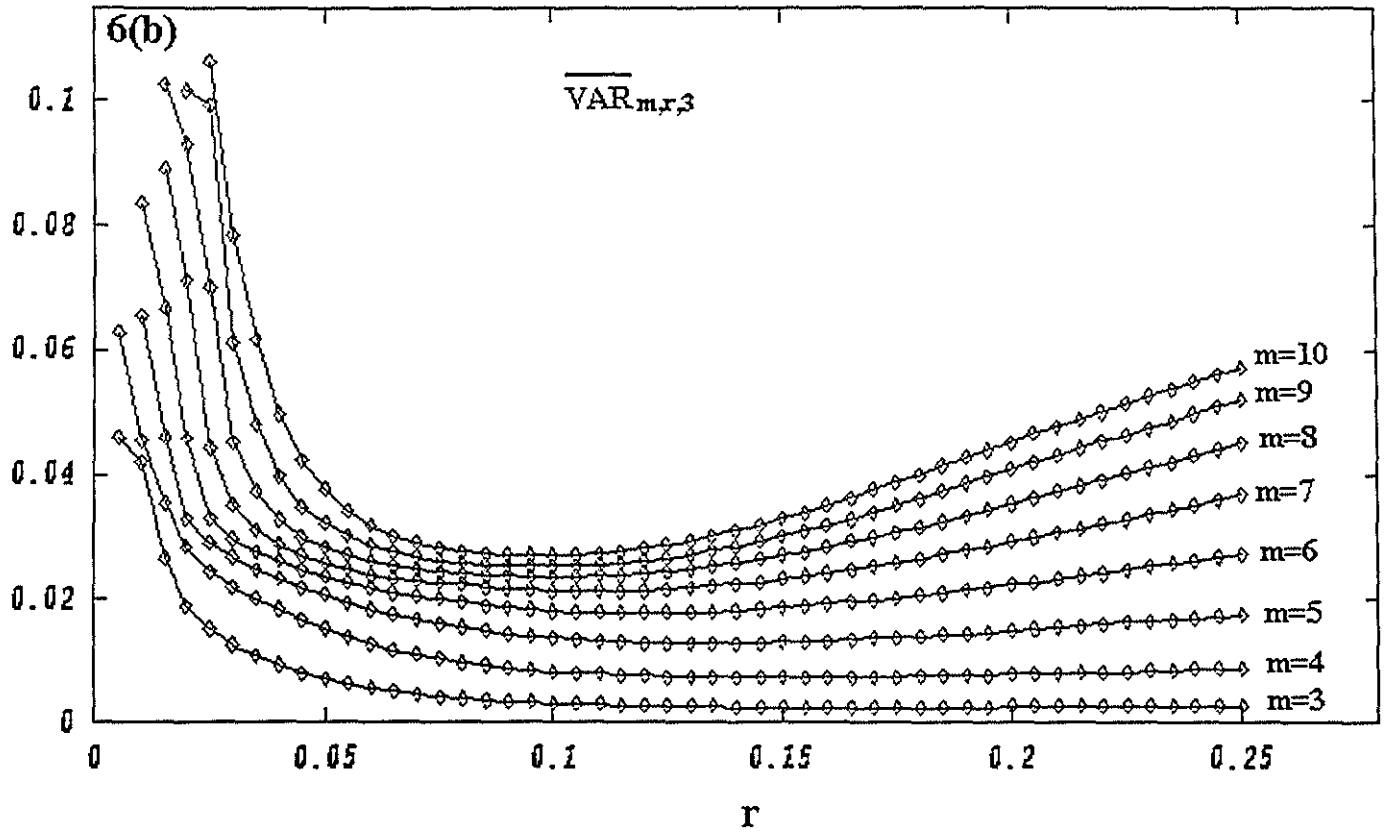
6(b)
$\overline{VAR}_{m,r,3}$
0.1
0.08
0.06
0.04
0.02
0
0
0.05
0.1
0.15
0.2
0.25
r
m=10
m=9
m=8
m=7
m=6
m=5
m=4
m=3

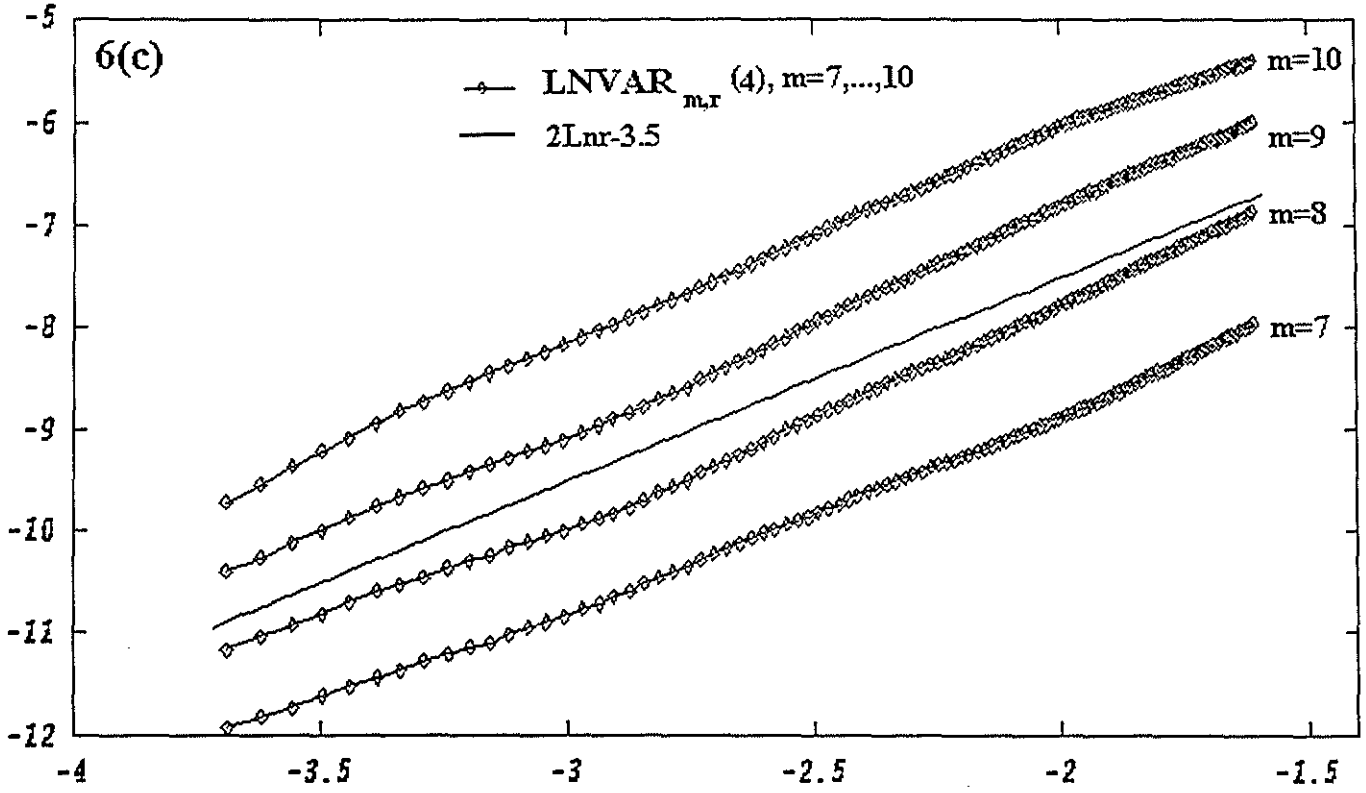
6(c)
LNVAR m,r (4), m=7,...,10
2Lnr-3.5
m=10
m=9
m=8
m=7
-5
-6
-7
-8
-9
-10
-11
-12
-4
-3.5
-3
-2.5
-2
-1.5

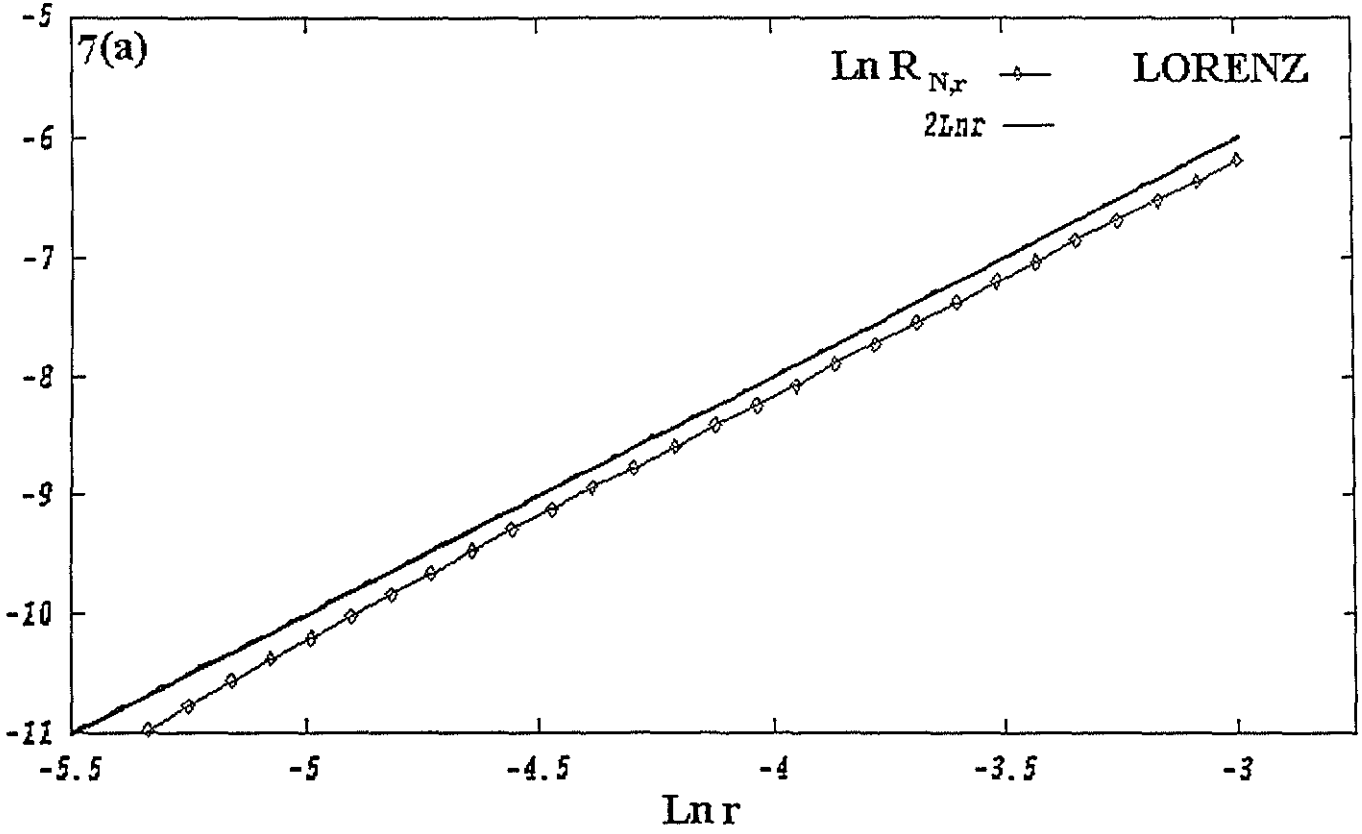
7(a)
Ln R N,r
LORENZ
2Lnr
-5
-6
-7
-8
-9
-10
-11
-5.5
-5
-4.5
-4
-3.5
-3
Ln r

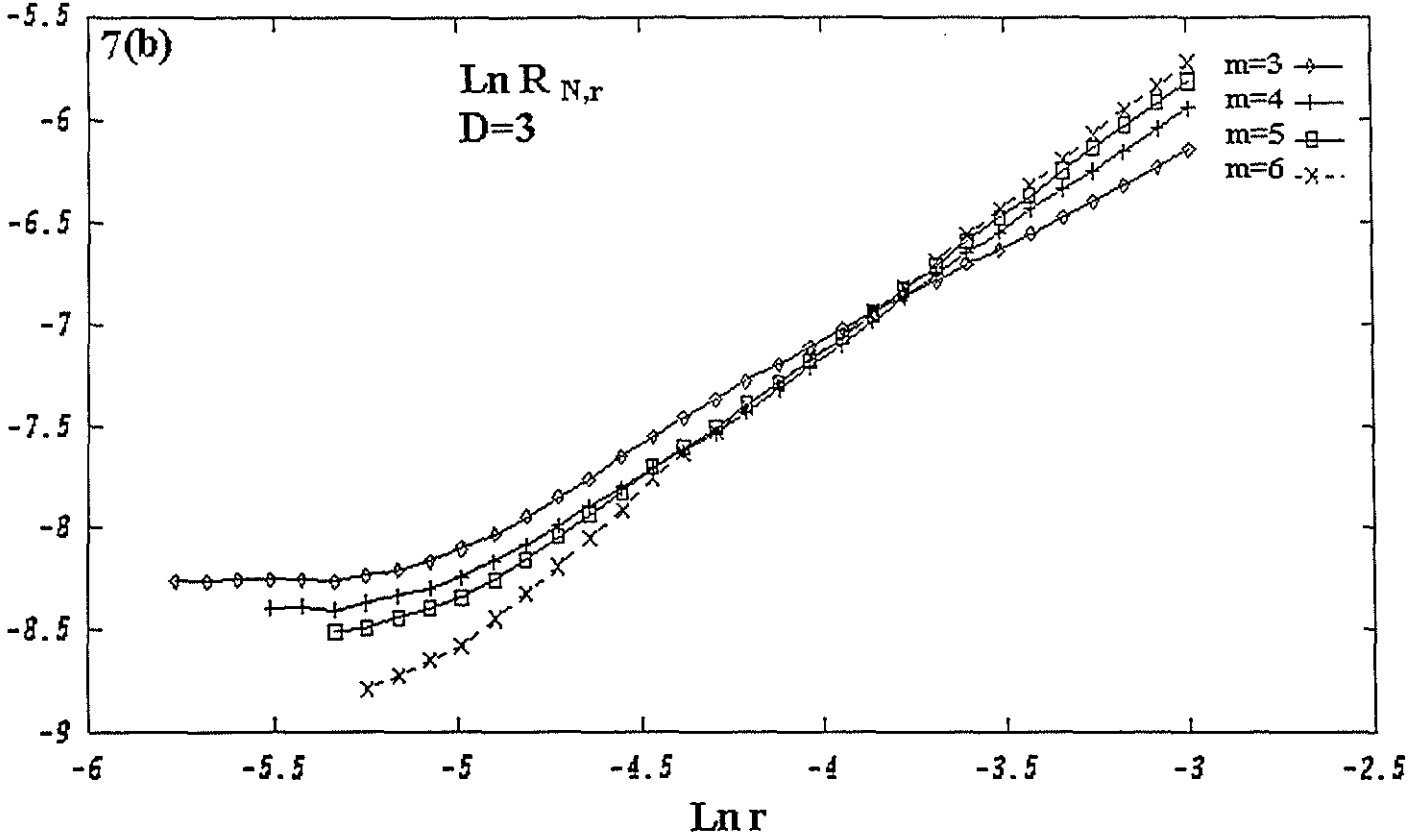
7(b)
Ln R N,r
D=3
m=3
m=4
m=5
m=6
-5.5
-6
-6.5
-7
-7.5
-8
-8.5
-9
-6
-5.5
-5
-4.5
-4
-3.5
-3
-2.5
Ln r

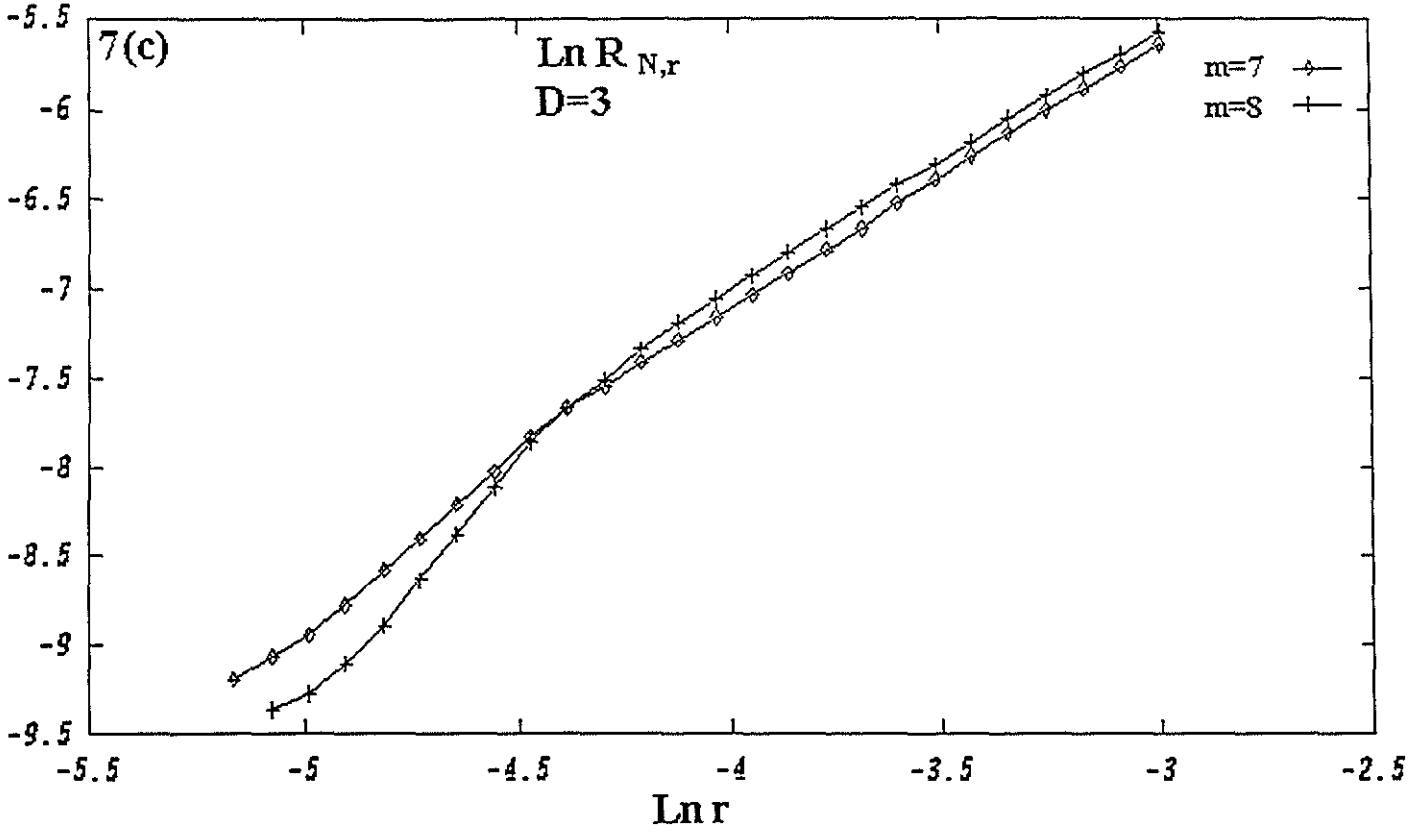
7(c)
Ln R N,r
D=3
m=7
m=8
-5.5
-6
-6.5
-7
-7.5
-8
-8.5
-9
-9.5
-5.5
-5
-4.5
-4
-3.5
-3
-2.5
Ln r

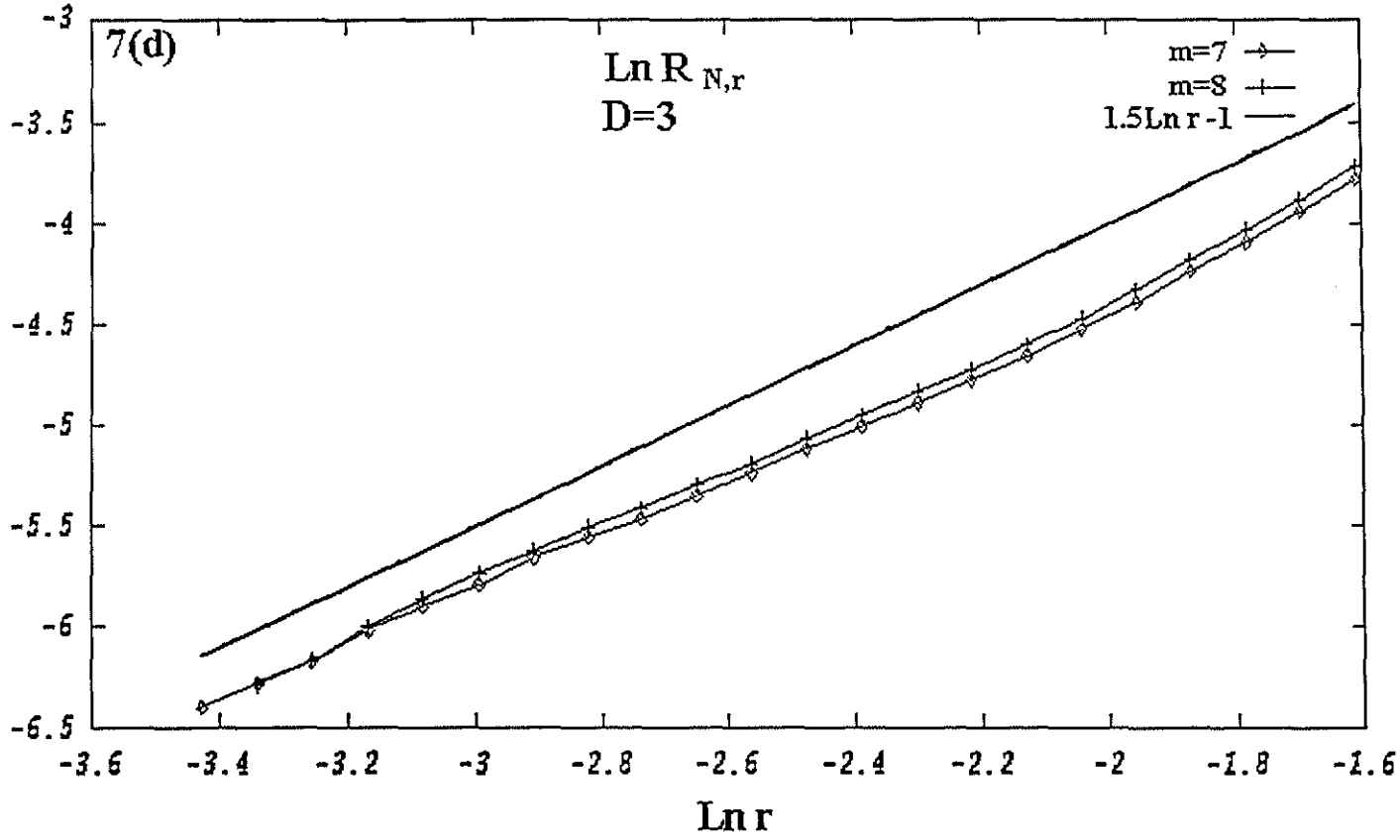
7(d)
Ln R N,r
D=3
m=7
m=8
1.5Ln r -1
-3
-3.5
-4
-4.5
-5
-5.5
-6
-6.5
-3.6
-3.4
-3.2
-3
-2.8
-2.6
-2.4
-2.2
-2
-1.8
-1.6
Ln r

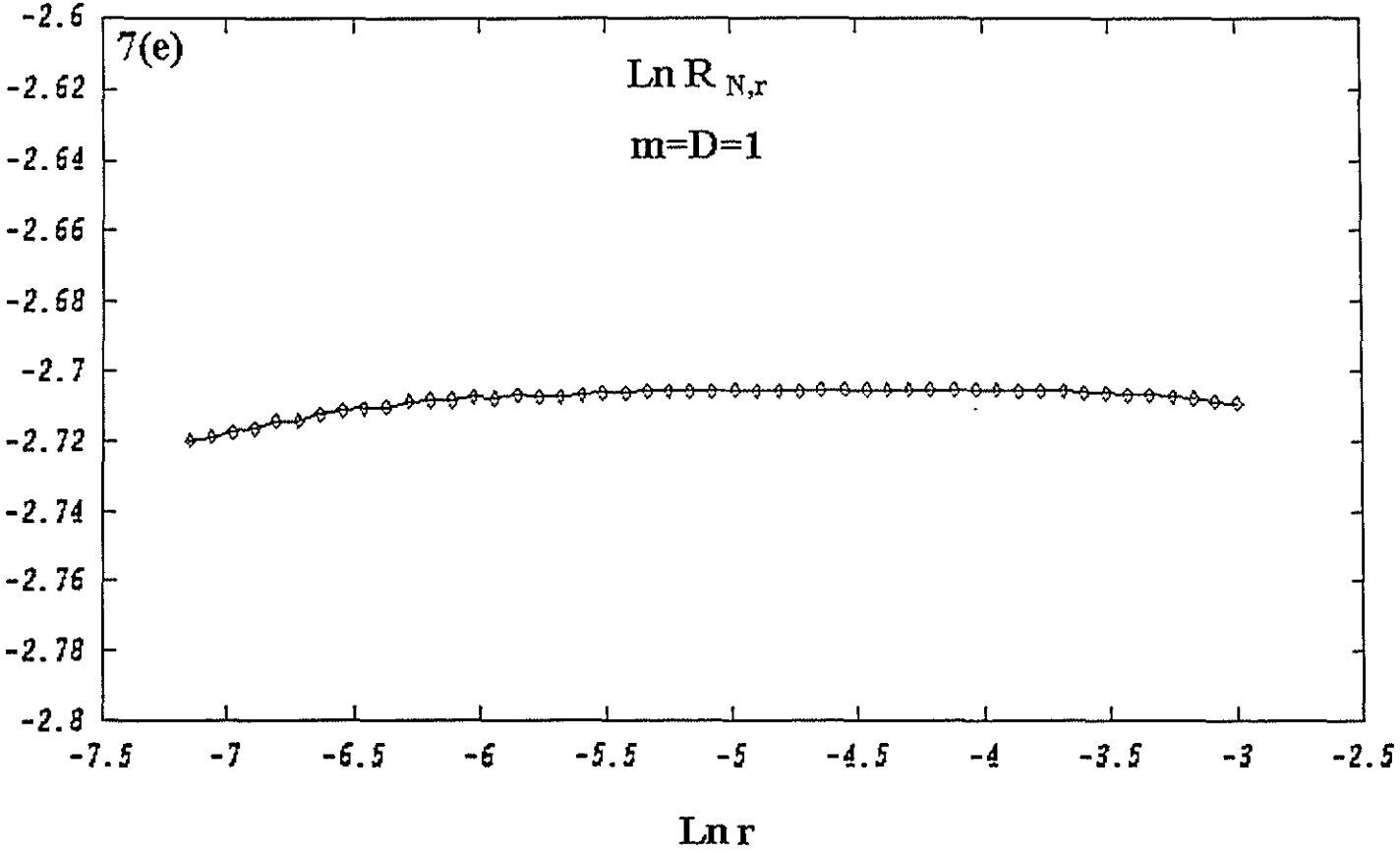
7(e)
Ln R N,r
m=D=1
-2.6
-2.62
-2.64
-2.66
-2.68
-2.7
-2.72
-2.74
-2.76
-2.78
-2.8
-7.5
-7
-6.5
-6
-5.5
-5
-4.5
-4
-3.5
-3
-2.5
Ln r

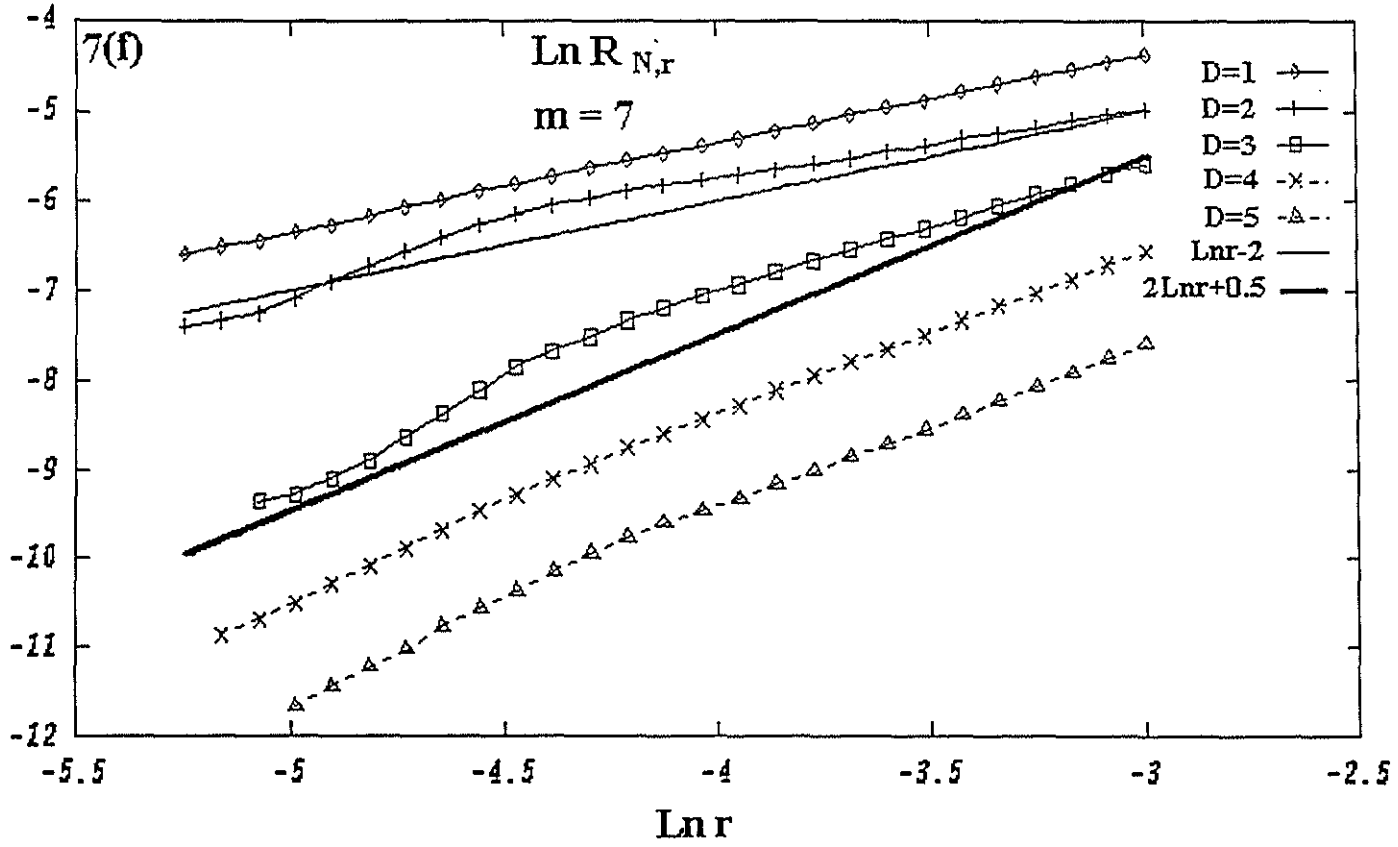
7(f)
Ln R N,r
m = 7
D=1
D=2
D=3
D=4
D=5
Lnr-2
2Lnr+0.5
-4
-5
-6
-7
-8
-9
-10
-11
-12
-5.5
-5
-4.5
-4
-3.5
-3
-2.5
Ln r

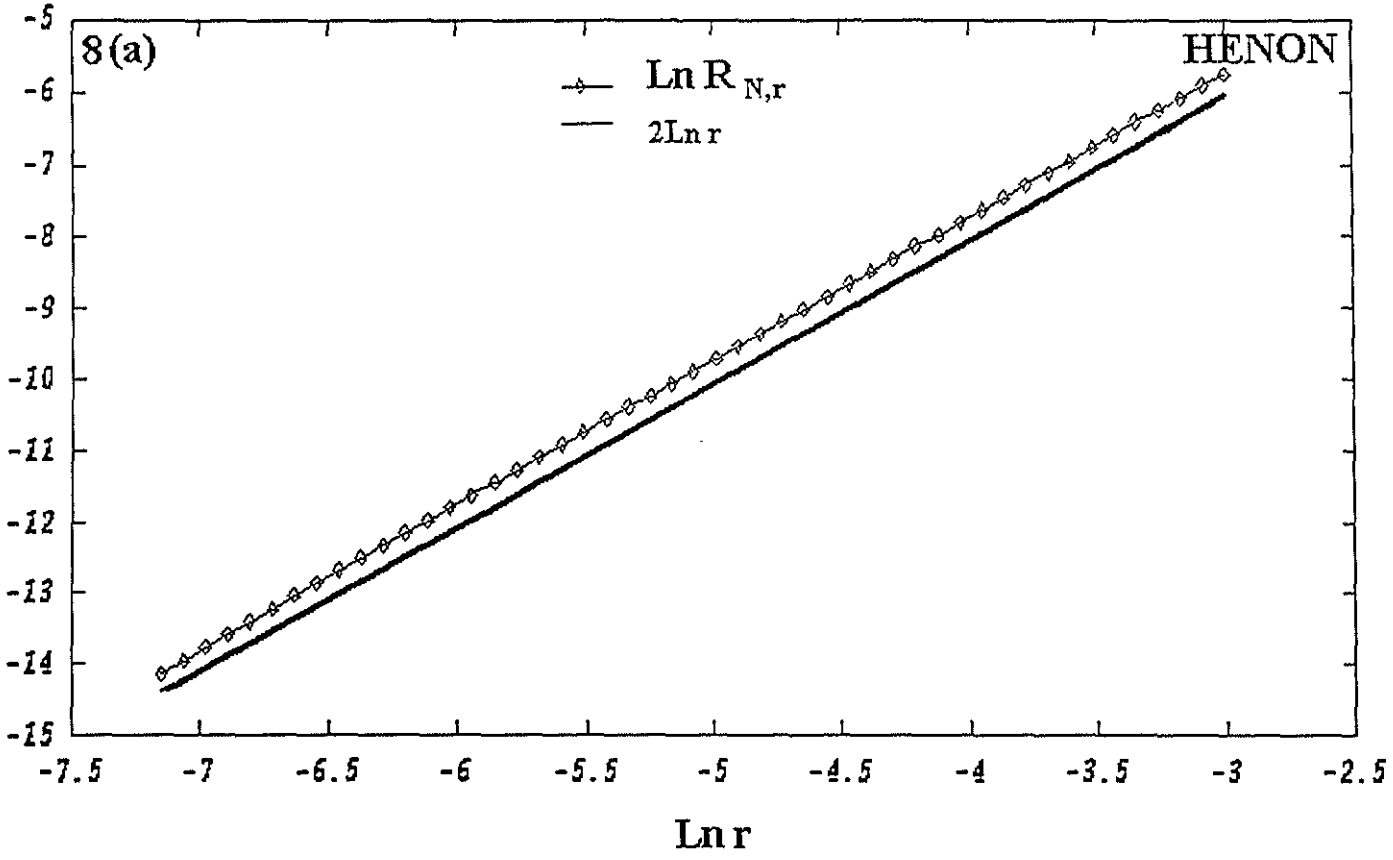
8(a)
HENON
Ln R N,r
2Ln r
-5
-6
-7
-8
-9
-10
-11
-12
-13
-14
-15
-7.5
-7
-6.5
-6
-5.5
-5
-4.5
-4
-3.5
-3
-2.5
Ln r

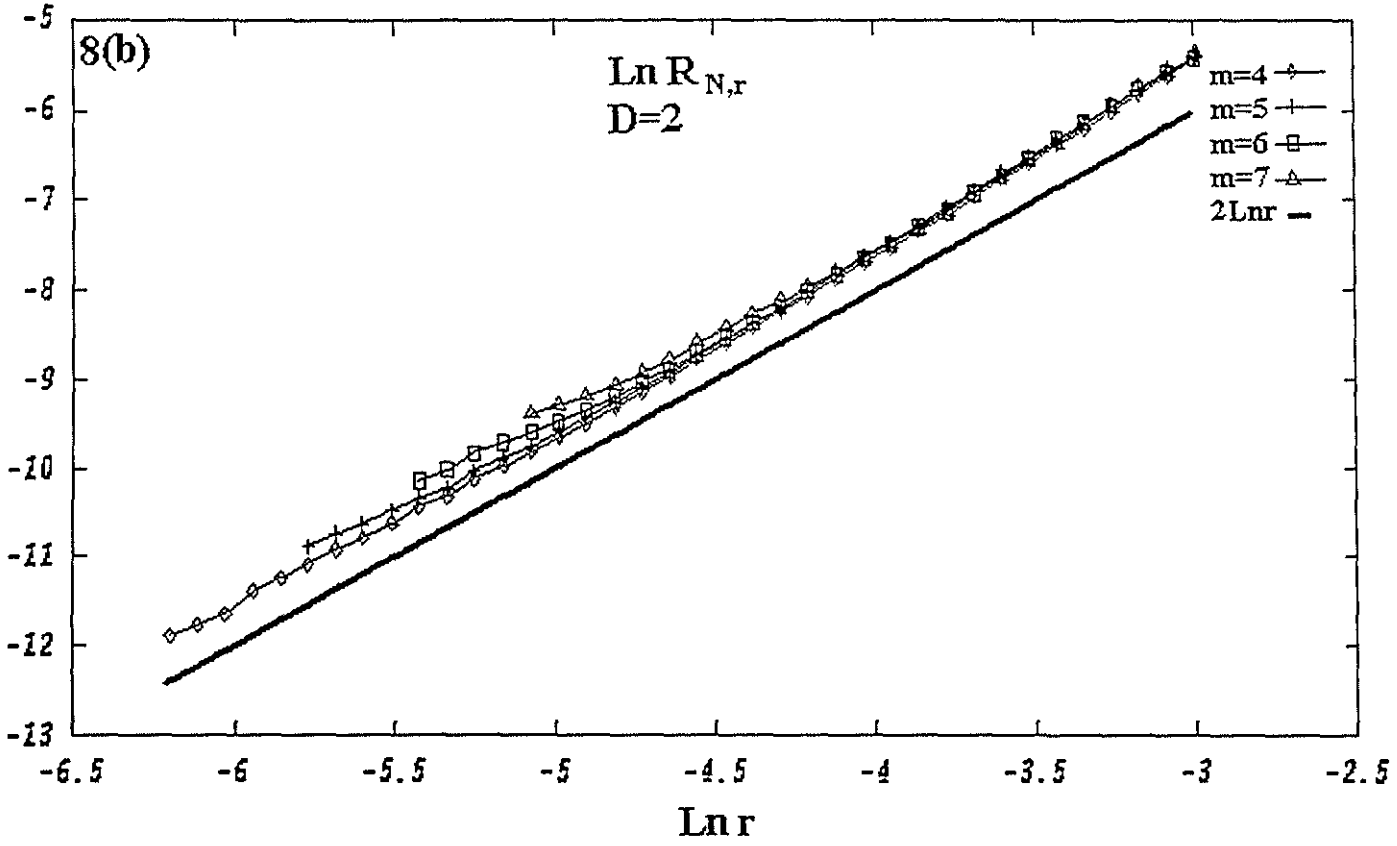
8(b)
Ln R N,r
D=2
m=4
m=5
m=6
m=7
2Lnr
-5
-6
-7
-8
-9
-10
-11
-12
-13
-6.5
-6
-5.5
-5
-4.5
-4
-3.5
-3
-2.5
Ln r

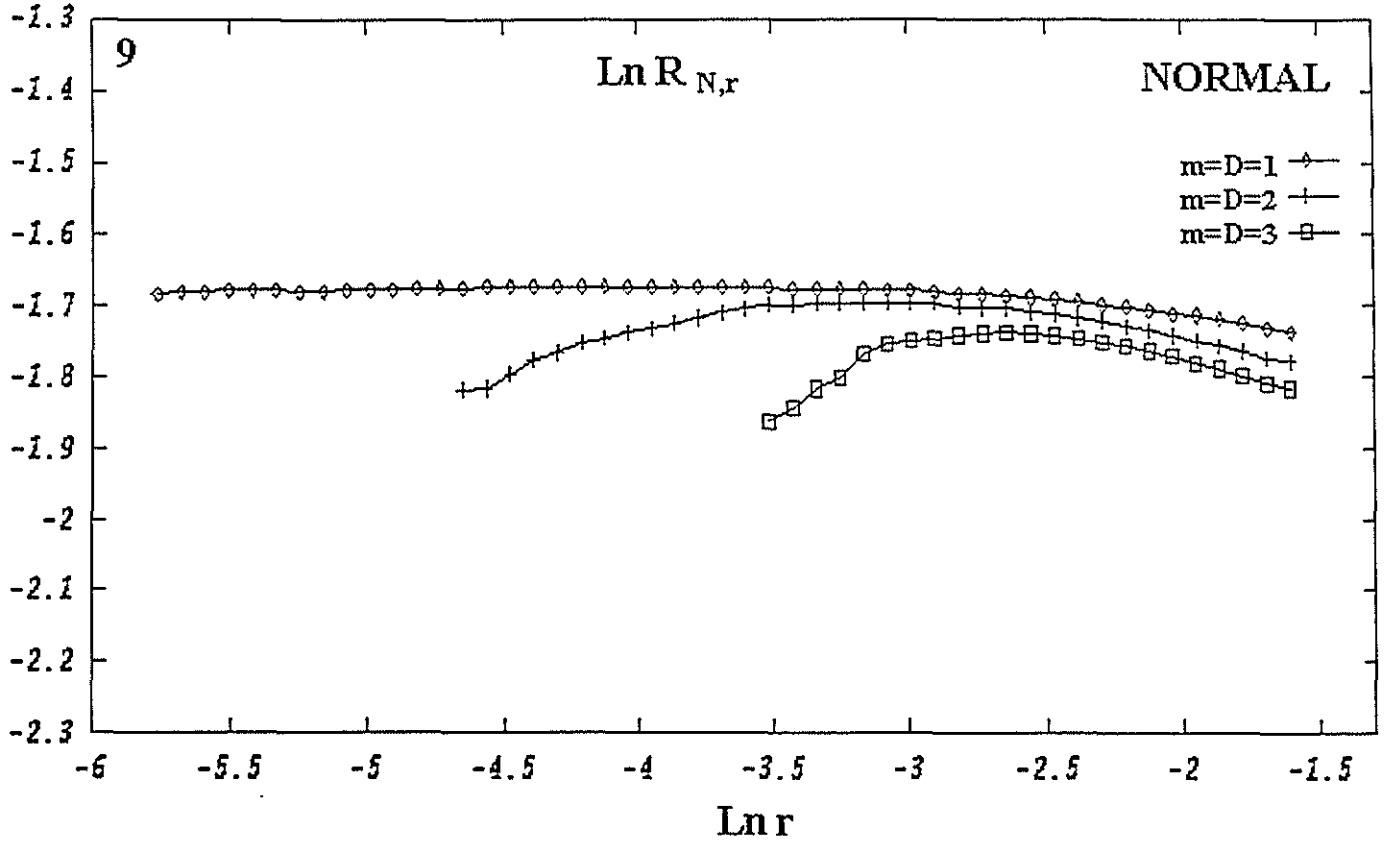
9
Ln R N,r
NORMAL
m=D=1
m=D=2
m=D=3
-1.3
-1.4
-1.5
-1.6
-1.7
-1.8
-1.9
-2
-2.1
-2.2
-2.3
-6
-5.5
-5
-4.5
-4
-3.5
-3
-2.5
-2
-1.5
Ln r